Journal of Visualized Experiments

Microelectrode array recording of sinoatrial node firing rate to identify intrinsic cardiac pacemaking defects in mice

--Manuscript Draft--

Article Type:	Invited Methods Collection - JoVE Produced Video
Manuscript Number:	JoVE62735R1
Full Title:	Microelectrode array recording of sinoatrial node firing rate to identify intrinsic cardiac pacemaking defects in mice
Corresponding Author:	Edward Glasscock Southern Methodist University Dallas, TX UNITED STATES
Corresponding Author's Institution:	Southern Methodist University
Corresponding Author E-Mail:	eglasscock@smu.edu
Order of Authors:	Praveen Kumar
	Man Si
	Kelsey Paulhus
	Edward Glasscock
Additional Information:	
Question	**Response**
Please indicate whether this article will be Standard Access or Open Access.	Standard Access (US$2,400)
Please specify the section of the submitted manuscript.	Medicine
Please indicate the **city, state/province, and country** where this article will be **filmed**. Please do not use abbreviations.	Dallas, TX USA
Please confirm that you have read and agree to the terms and conditions of the author license agreement that applies below:	I agree to the Author License Agreement
Please provide any comments to the journal here.	our manuscript shows suggested script highlighted in yellow with text edits in red lettering
Please indicate whether this article will be Standard Access or Open Access.	Standard Access ($1400)

TITLE:

Microelectrode Array Recording of Sinoatrial Node Firing Rate to Identify Intrinsic Cardiac Pacemaking Defects in Mice

AUTHORS AND AFFILIATIONS:

Praveen Kumar[1], Man Si[1], Kelsey Paulhus[1], and Edward Glasscock[1]

[1]Department of Biological Sciences, Southern Methodist University, Dallas TX

Corresponding Author
Edward Glasscock (eglasscock@smu.edu)

Email Addresses of Co-Authors:
Praveen Kumar (praveenk@smu.edu)
Man Si (msi@smu.edu)
Kelsey Paulhus (kpaulhus@smu.edu)

KEYWORDS:

microelectrode array, sinoatrial node, pacemaking, firing rate, intrinsic cardiac pacemaking, intrinsic firing rate

SUMMARY:

This protocol aims to describe a new methodology to measure intrinsic cardiac firing rate using microelectrode array recording of the whole sinoatrial node tissue to identify pacemaking defects in mice. Pharmacological agents can also be introduced in this method to study their effects on intrinsic pacemaking.

ABSTRACT:

The sinoatrial node (SAN), located in the right atrium, contains the pacemaker cells of the heart, and dysfunction of this region can cause tachycardia or bradycardia. Reliable identification of cardiac pacemaking defects requires the measurement of intrinsic heart rates by largely preventing the influence of the autonomic nervous system, which can mask rate deficits. Traditional methods to analyze intrinsic cardiac pacemaker function include drug-induced autonomic blockade to measure *in vivo* heart rates, isolated heart recordings to measure intrinsic heart rates, and sinoatrial strip or single-cell patch-clamp recordings of sinoatrial pacemaker cells to measure spontaneous action potential firing rates. However, these more traditional techniques can be technically challenging and difficult to perform. Here, we present a new methodology to measure intrinsic cardiac firing rate by performing microelectrode array (MEA) recordings of whole-mount sinoatrial node preparations from mice. MEAs are composed of multiple microelectrodes arranged in a grid-like pattern for recording *in vitro* extracellular field potentials. The method described herein has the combined advantage of being relatively faster, simpler, and more precise than previous approaches for recording intrinsic heart rates, while also allowing easy pharmacological interrogation.

INTRODUCTION:

The heart is a complex organ governed by both cardiac-intrinsic and extrinsic influences such as those that originate in the brain. The sinoatrial node (SAN) is a defined region in the heart that houses the pacemaker cells (also referred to as sinoatrial cells, or SA cells) responsible for the initiation and perpetuation of the mammalian heartbeat[1,2]. The intrinsic heart rate is the rate driven by the pacemaker cells without influence by other cardiac or neuro-humoral influences, but traditional measures of heart rate in humans and live animals, such as electrocardiograms, reflect both the pacemaker and neural influences on the heart. The most notable neural influence on SA cells is from the autonomic nervous system, which constantly modulates firing patterns to meet the physiological requirements of the body[3]. Supporting this idea, both sympathetic and parasympathetic projections can be found near the SAN[4]. The intrinsic cardiac nervous system (ICNS) is another important neural influence where ganglionated plexi, specifically in the right atria, innervate and regulate the activity of the SAN[5,6].

Understanding pacemaking deficits is clinically important, as dysfunction can underlie many cardiac disorders, as well as contribute to the risk of other complications. Sick sinus syndrome (SSS) is a category of diseases characterized by dysfunction of the sinoatrial node which impedes proper pacemaking[7,8]. SSS can present with sinus bradycardia, sinus pauses, sinus arrest, sinoatrial exit block, and alternating bradyarrythmias and tachyarrhythmias[9] and can lead to complications including increased risk of embolic stroke and sudden death[8,10]. Those with Brugada syndrome, a cardiac disorder marked by ventricular fibrillation with an increased risk of sudden cardiac death, are at greater risk for arrhythmogenic events if they also have comorbid SAN dysfunction[11,12]. Sinoatrial dysfunction may also have physiological consequences beyond the heart. For example, SSS has been observed to trigger seizures in a patient due to cerebral hypoperfusion[13].

To identify sinoatrial pacemaking deficits, intrinsic heart rates need to be determined by measuring the activity of the SAN without the influence of the autonomic nervous system or humoral factors. Clinically, this can be approximated by pharmacological autonomic blockade[14], but this same technique can also be applied in mammalian models to study intrinsic cardiac function[15,16]. While this approach blocks a large portion of contributing neural influences and allows for *in vivo* cardiac examination, it does not completely eliminate all extrinsic influences on the heart. Another research technique used to study intrinsic cardiac function in animal models is isolated heart recordings using Langendorff-perfused hearts, which typically involve measurements using electrograms, pacing, or epicardial multielectrode arrays[17–20]. While this technique is more specific to cardiac function since it involves removing the heart from the body, the measurements may still be influenced by mechano-electric autoregulatory mechanisms that could influence intrinsic heart rate measurements[21]. The isolated heart recordings may also still be influenced by autonomic regulation through the ICNS[5,6,22,23]. Furthermore, maintaining a physiologically relevant temperature of the heart, which is critical for cardiac function measurements, can be difficult in isolated heart approaches[20]. A more direct method to study SAN function is to specifically isolate SAN tissue and measure its activity. This can be accomplished through SAN strips (isolated SAN tissue) or isolated SAN pacemaker cells[24,25]. Both require a high degree of technical training, as the SAN is a very small and highly defined region,

and cell isolation poses an even greater challenge as dissociation can damage the overall health of the cell if not performed correctly. Furthermore, these techniques require expert electrophysiological skills in order to successfully record from the tissue or cells using individual recording microelectrodes.

In this protocol, we describe a technique to record the SAN *in vitro* by using a microelectrode array (MEA) to obtain intrinsic heart rate measurements. This approach has the advantage of making highly specific electrophysiological recordings accessible to researchers lacking intensive electrophysiological skillsets. MEAs have previously been used to study cardiomyocyte function in primary cardiomyocyte cultures[26–32], cardiac sheets[33–39], and tissue whole mounts[40–47]. Previous work has also been done to examine field potentials in SAN tissue[41,42]. Here, we provide a methodology to use the MEA to record and analyze murine intrinsic SAN firing rates. We also describe how this technique can be used to test pharmacological effects of drugs on SAN intrinsic firing rates by providing a sample experiment showing the effects of 4-aminopyridine (4-AP), a voltage-gated K^+ channel blocker. Using defined anatomical landmarks, we can accurately record the SAN without having to perform the extensive tissue dissections or cell isolations required in other methods. While the MEA can be cost-prohibitive, the recordings provide highly specific and reliable measures of pacemaking that can be used in a vast array of clinical and physiological research applications.

PROTOCOL:

All experimental procedures described here have been carried out in accordance with the guidelines of the National Institutes of Health (NIH), as approved by the Institutional Animal Care and Use Committee (IACUC) at Southern Methodist University.

1. Coating the multielectrode array (MEA) for recording

1.1. Make 25 mM borate buffer.

1.1.1. Dissolve 0.953 g of $Na_2B_4O_7 \cdot 10\ H_2O$ in 80 mL of distilled water.

1.1.2. Adjust the pH to 8.4 with HCl and then add distilled water to a final volume of 100 mL.

1.2. Make a 0.1% stock solution of polyethyleneimine (PEI).

1.2.1. Add 100 µL of 50% (w/v) PEI to 4.9 mL of distilled water to make a 1% PEI solution.

1.2.2. Dilute the 1% PEI solution to 0.1% in borate buffer by adding 1 mL of the 1% PEI solution to 9 mL of the 25 mM borate buffer.

1.3. Pipette ~1 mL of the 0.1% PEI solution into the microelectrode array (MEA) dish so that the electrodes are completely covered (**Figure 1A and 1B**).

NOTE: The microelectrodes of the MEA are typically composed of platinum black or carbon

nanotube and insulated with polyimide (or acrylic); both materials are hydrophobic. By coating the MEA with a cationic polymer such as PEI, the hydrophobic MEA surface is made more hydrophilic, allowing tissue samples to make better contact with the MEA surface (**Figure 1A1**).

1.4. Cover the MEA dish with thermoplastic film to reduce evaporation and leave the MEA overnight at room temperature (**Figure 1C**).

1.5. Aspirate the PEI solution from the MEA dish using a pipette, being careful not to touch the electrode grid which can damage the electrodes, and then rinse ≥4 times with distilled water (**Figure 1D**).

1.6. Store the PEI-coated MEA under 1-2 mL of ultrapure water and sealed with thermoplastic film at 4 ˚C until needed. Alternatively, store the coated MEA by submerging it in a beaker filled with ultrapure water (**Figure 1E**).

NOTE: The PEI coating process only needs to be performed once for the MEA before its first use, and after each recording session, the MEA should be stored submerged in ultrapure water.

2. Preparing complete Tyrode's solution for tissue dissection

2.1. Make 1,000 mL of complete Tyrode's solution for dissection; first, add 8.1816 g of NaCl to 800 mL of ultrapure water.

2.2. Add the following amount of chemicals to the solution: 0.4025 g of KCl; 0.1633 g of KH_2PO_4; 1.1915 g of HEPES; 0.9999 g of glucose; 0.0952 g of $MgCl_2$; 0.2646 g of $CaCl_2{\cdot}2H_2O$.

2.3. Adjust the pH to 7.4 with NaOH and then add ultrapure water until the total volume is 1,000 mL.

NOTE: The final composition of the Complete Tyrode's solution will be the following (in mM): 140 NaCl, 5.4 KCl, 1.2 KH_2PO_4, 5 HEPES, 5.55 glucose, 1 $MgCl_2$, 1.8 $CaCl_2$.

3. Preparing oxygenated Tyrode's solution for recording

3.1. Make 500 mL of Tyrode's solution; add 4.003 g of NaCl to 400 mL of ultrapure water.

3.2. Add the following amounts of chemicals to the solution: 0.651 g of $NaHCO_3$; 0.042 g of NaH_2PO_4; 0.132 g of $CaCl_2{\cdot}2H_2O$; 0.149 g of KCl; 0.0476 g of $MgCl_2$; 0.999 g of glucose.

3.3. Adjust the pH to 7.4 with HCl and then add ultrapure water until the total volume is 500 mL.

3.4. Oxygenate the solution with carbogen for at least 30 min at room temperature before starting the recording.

NOTE: The final composition of the Tyrode's solution will be the following (in mM): 137 NaCl, 15.5 $NaHCO_3$, 0.7 NaH_2PO_4, 1.8 $CaCl_2$, 4 KCl, 1 $MgCl_2$, 11.1 glucose. This Tyrode's solution has a slightly different composition from the Complete Tyrode's solution used for dissection.

4. **Preparing 4-aminopyridine (4-AP) solution for pharmacological modulation**

4.1. Make a 1 mM working solution of 4-AP; add 18.82 mg of 4-AP to 200 mL of the Tyrode's solution from step 3.

4.2. Oxygenate the 4-AP solution for at least 30 min before the experiment.

5. **Preparing the Petri dish for dissection**

5.1. Mix silicone elastomer components in a 10:1 ratio (by weight) of the base to curing agent.

5.2. Pour ~15 mL of silicone elastomer mixture into a 60 mm diameter Petri dish.

5.3. Allow elastomer to cure at room temperature for 48 h before use.

NOTE: The siliconized Petri dish can be reused for future dissections.

6. **Dissecting the sinoatrial node (SAN)**

6.1. Prepare heparinized Complete Tyrode's solution for SAN dissection.

6.1.1. Add 400 µL of heparin (1,000 USP/mL) to 40 mL of Complete Tyrode's solution and warm in a 37 ˚C water bath.

6.2. Inject the mouse intraperitoneally with 200-300 µL of heparin (1000 USP/mL) and allow the animal to sit for 10 min.

6.3. Euthanize the heparinized mouse by isoflurane overdose.

6.3.1. Place the mouse in a small glass chamber that contains isoflurane vapors generated by adding 200-300 µL of liquid isoflurane to a filter paper inside a perforated plastic tube.

NOTE: Because isoflurane can cause skin irritation and can also be absorbed through the skin, the liquid should not contact the mouse directly. Therefore, the isoflurane-soaked wipe is placed in a perforated tube for administration.

6.3.2. Verify death by cessation of movement and breathing effort and by the absence of a toe pinch reflex. Death usually takes about 1-2 min following placement into the chamber.

NOTE: Death is usually accompanied by urination.

6.4. Place the mouse in a supine position on a dissection board with paws outstretched and fix the paws to the board using 1 inch long, 23-gauge syringe needles. Then remove the fur in the vicinity of the bottom of the rib cage by using surgical scissors and cutting the fur at the roots.

NOTE: For a dissection board, polystyrene cooler lids can be used.

6.5. While holding the skin with a hemostat, use surgical scissors to make a transverse incision in the skin just beneath the bottom of the rib cage from about the left costal arch to the right costal arch (**Figure 3A**).

6.6. Cut open the peritoneum with surgical scissors and carefully separate the liver from the diaphragm, being careful not to nick the liver, which will cause excessive bleeding (**Figure 3B**). Incise the diaphragm along the thorax to expose the thoracic cavity (**Figure 3C-D**).

6.7. Using surgical scissors, cut the lateral walls of the rib cage from the edges of the costal arches up to the clavicles to expose the heart, being careful to avoid damaging the heart (**Figure 3D**). Then use a 23-gauge syringe needle to pin the rib cage over the shoulder, holding it in place and out of the way of the surgical field.

6.8. Use a transfer pipette to drip warm (37 ˚C) heparinized Complete Tyrode's solution onto the heart to keep it moist.

NOTE: Do not allow the heart to dry out.

6.9. Remove the lungs by holding them with extra fine Graefe forceps and severing the trachea with surgical scissors (**Figure 3E**).

6.10. Hold the apex of the heart with extra fine Graefe forceps and remove it by cutting the aorta and inferior vena cava with surgical scissors. Transfer the heart to a Petri dish containing cured silicone elastomer (**Figure 4A**) and use a transfer pipette to bathe the heart with 2-3 mL of warm (37 ˚C) heparinized Complete Tyrode's solution.

NOTE: Be careful not to damage the delicate posterior wall of the right atria, which contains the SAN, and the connected right atrial veins. Bathing the heart with Complete Tyrode's solution keeps the heart from drying out but do not fully submerge the heart in solution as it will impair visibility during dissection.

6.11. Orient the heart with the right atrium on the experimenter's right and the left atrium on the experimenter's left.

NOTE: Dissection of the SAN tissue should be done quickly in order to prevent ischemia-related injury.

6.12. Attach the apex of the heart to the dish with a dissection pin. Then, while holding the inferior vena cava with Dumont #2 laminectomy forceps, insert a 22 G syringe needle through the inferior and superior vena cava to locate their position in the right atrium, which also identifies the approximate position of the SAN (located in the patch of tissue between the inferior and superior vena cava (**Figure 4B**)).

6.13. Using small dissection pins, pin the left and right atrial appendages to the dish.

6.13.1. While holding the left atrial appendage with Dumont #2 laminectomy forceps, put a dissection pin through the left atrial appendage to hold it in place.

6.13.2. While holding the right atrial appendage with Dumont #55 forceps, put a dissection pin through the right atrial appendage to hold it in place.

NOTE: The same type of forceps can be used to hold the left and right atrial appendages if desired.

6.14. Remove the syringe needle that spans the venae cavae.

6.15. To release blood from the heart, use Castroviejo scissors to remove the apex of the heart (i.e., the bottom half) by making a transverse incision across the ventricles (**Figure 4C**). Then, wash the heart by adding warm (37 ˚C) heparinized Complete Tyrode's solution with a transfer pipette.

6.16. Use Castroviejo scissors to cut along the atrioventricular septum keeping the incision closer to the ventricle than the atria. Continue cutting along the atrioventricular septum until the atria are separated from the ventricles.

6.17. Cut along the interatrial septum to remove the left atrium.

6.18. Place dissection pins in the periphery of the right atrium to make it lay flat (**Figure 4D**). Remove any remaining fat, vessels, or tissue from the atrium using the Castroviejo scissors.

6.19. Locate the SAN in the right atrium, which in this orientation is approximately bordered by the superior vena cava (on the top), inferior vena cava (on the bottom), and cristae terminalis (on the left) (**Figure 4D**).

NOTE: The crista terminalis appears as a dark muscular ridge between the right atrial appendage and the SAN. Often the SAN artery can also be seen coursing through the SAN (**Figure 4D**).

7. Preparing the MEA system for recording

7.1. Add Tyrode's solution (from step 3) to the input solution bottle (**Figure 5C**) and oxygenate it by turning on the flow of carbogen gas (**Figure 5A**) to the system.

NOTE: The Tyrode's solution used for the recording is slightly different in composition from the Complete Tyrode's solution used for the dissection.

7.2. Verify the flow of carbogen by observing bubbles in the conical flask, which is used to humidify the gas (**Figure 5B**), and the input solution bottle (**Figure 5C**)**.**

7.3. Insert the peristaltic pump inflow tubing (**Figure 5D**) into the Tyrode's recording solution (**Figure 5C**). Then, insert the peristaltic pump outflow tubing into the collection bottle (**Figure 5I**).

7.4. Set the peristaltic pump to 25 rpm, which gives a flow rate of 2 mL/min and start the pump. Check the system for any buffer leakage or overflow.

7.5. Set the temperature controller to 37 ˚C, the physiological temperature of mice (**Figure 5E**).

8. Placing the heart tissue on the MEA grid

8.1. Transfer the dissected SAN tissue with the help of a paint brush (**Figure 6A**) from the dissecting Petri dish onto the MEA grid (**Figure 1A1**).

8.1.1. While looking under an inverted microscope, gently position the tissue with a soft paint brush so that the SAN region overlays the electrode grid.

8.1.2. Re-position the tissue as necessary to ensure it lays flat on the electrode grid, making good contact with the electrodes.

NOTE: A soft paint brush is required for moving the tissue to avoid damaging the electrode grid.

8.2. Once the tissue is correctly positioned, use bone forceps (or any curved forceps) to place the mesh over the tissue (**Figure 6A**)**.** Then use the bone forceps to place the harp anchor (**Figure 6A**) on the mesh to hold everything in place (**Figure 6B**).

8.3. Take a picture of the positioning of the tissue on the MEA so that the activity of individual electrodes can be correlated with their anatomical location during the recording. This can be done by holding a smartphone up to the inverted microscope objective or by using an attached microscope camera.

NOTE: If the orientation of the MEA is not changed after taking the picture, the top left electrode will appear as the first channel (Ch1) during recording.

8.4. Place the MEA dish on the connector plate (**Figure 5F and 6C**) and carefully place the perfusion cap (**Figure 6C**) on the MEA dish without disturbing the harp slice anchor. The perfusion cap can be further secured using a piece of lab tape (**Figure 6C**).

NOTE: In addition to having adjustable solution inflow and outflow pipes, the cap also has a port

for the delivery of gas (**Figure 6C**). In addition, the reference electrode ring runs through the cap (**Figure 6C**).

8.5. Allow the tissue to recover from handling and to acclimate to the chamber for 15-20 min prior to recording.

9. Setting the data acquisition protocol for recording

NOTE: The following steps describe opening the software protocol for spontaneous beat recording and defining the recording conditions. The specifics of these steps may vary depending on the specific software being used, but the general outline should remain the same.

9.1. Turn on the amplifier (**Figure 5G**), and set up a workflow for the recording in the software on the computer (**Figure 5H**).

9.1.1. Open the software and click on the **Workflow**.

9.1.2. Select **Open New Folder**.

9.1.3. Open the **From Templates** folder.

9.1.4. Select **64MD1-1920X1080** (depending on the resolution of your desktop).

9.1.5. Open the **QT** folder.

9.1.6. Open the **Spontaneous recording** folder.

9.1.7. Select **Beat_recording.moflo** template and open it (**Figure 7A**).

9.2. Set the recording parameters to specify the number of traces, trace duration, trace interval, input voltage, sampling rate, etc., according to the desired recording conditions (**Figure 7B**).

NOTE: For beat frequency and interspike data acquisition, typically use an input range voltage of 2.9 mV, a 1-Hz high pass filter, a 1000-Hz low pass filter, and a sampling rate of 20 kHz.

9.3. To mark different phases or conditions of the experiment, such as before and after drug administration, click on the **Annotations** tab to add the desired notations (**Figure 7C**).

9.4. To specify the file destination for the data to be collected, select the **Enable Storage** box and enter the desired file name in the **File name modifier** box.

10. Performing the recording and collecting data

10.1. Click the **Record and Play** button on the topmost menu bar of the acquisition software to

start the recording. Acquire data for 10 traces of 1 min duration with intervals of 2 min between traces.

10.2. From these initial traces, verify that the recorded waveforms are consistent with a healthy and high-quality tissue preparation by confirming that the majority of the recording channels exhibit signal amplitudes of ≥ 0.5 mV and identical inter-spike intervals (**Figure 8**).

NOTE: An initial assessment of the activity and waveforms of the individual microelectrodes corresponding to their anatomical locations can be performed by referencing the picture acquired after positioning the tissue on the MEA.

10.3. To measure the effects of drugs on the tissue, pause the recording after acquiring initial baseline data by clicking the pause button on the topmost menu bar.

NOTE: The drug response phase of the experiment can be notated in the recording by clicking on the **Annotations** tab and adding the desired notation as described above (**Figure 7C**).

10.4. Pause the pump and switch the pump inflow tubing from the normal recording solution to Tyrode's solution containing the desired drug of choice.

NOTE: In the example experiment, Tyrode's solution was used with 1 mM 4-aminopyridine (4-AP).

10.5. Restart the pump and un-pause the recording to begin collecting data again.

10.6. Once the drug-infused Tyrode's solution has reached the tissue, record 10 traces in the same manner as done previously for the baseline recordings.

NOTE: The traces will take some time to stabilize as the drug infuses into the recording chamber. The mechanism of action of the drug may also affect recording stability. For drugs that have reversible mechanisms of action, a washout period should also be recorded to confirm restoration of activity to baseline levels, which is an indicator of healthy tissue.

10.7. Click **Stop** to conclude the recordings.

10.8. Take a final picture of the positioning of the tissue on the MEA under the microscope in case the tissue has shifted following the initial recording setup procedure.

11. Cleaning the setup after the recording

11.1. Clean the MEA.

11.1.1. After finishing recording, gently remove the recording solution from the MEA dish using a 1 mL micropipette.

NOTE: Be careful not to contact the MEA electrodes which can damage them.

11.1.2. Remove the mesh and harp anchor with bone forceps (or any curved forceps). Then use a paint brush to dislodge the tissue from the MEA surface always being careful not to touch the individual microelectrodes.

11.1.3. Using a wash bottle, gently rinse the MEA dish with ultrapure water about 3 to 4 times.

11.1.4. Store the cleaned MEA immersed in ultrapure water at 4 ˚C.

11.2. Rinse the system tubing by running ultrapure water through it for at least 5 min using the maximum speed setting on the peristaltic pump.

NOTE: To prevent fungal growth, no water or buffer solution should be left inside the tubing after cleaning.

12. Analyzing the MEA recordings to measure SAN beat frequency

12.1. Open the saved recorded data file in the "Beat_frequency_analysis" template of the analysis software (**Figure 9**).

12.2. Click on the **Play** button and allow the entire recording to run to visualize the data set and assign appropriate analysis parameters.

12.2.1. Select the binning window for the desired display format of the data, whether it is displayed as an average per trace or average per time (**Figure 10A**).

12.2.2. Select the channels to be included in the analysis and set the desired amplitude maxima or amplitude minima threshold values for automated waveform peak identification (**Figure 10B**).

NOTE: An individual channel, a combination of channels, or all 64 channels can be selected for analysis at this step (**Figure 9**). If the threshold values selected are too close to the waveform's maxima and minima values, some waveform peaks may not be identified by the analysis software.

12.2.3. Set the amount of pre-spike and post-spike time to be included in the analysis.

NOTE: Settings of 50 ms pre-spike and 100 ms post-spike usually work well (**Figure 10B**).

12.3. After setting the analysis conditions, click on the Play button again to rerun the data set and confirm that the analysis parameters are appropriate for spike extraction.

12.4. For analysis, identify the three most stable consecutive traces that exhibit stable beating

rate for each trace across the majority of channels both during the baseline period of the experiment and another three consecutive stable traces during the drug exposure period (**Figure 10A**).

12.5. Specify the start and end traces for analysis and enter the time duration of each trace to be analyzed (**Figure 9**).

12.6. Before starting the analysis, select the enable boxes for both **Save beat per minute** and **Save interspike interval** (**Figure 10B**).

12.7. Enter the desired file name in the **File name modifier** box (**Figure 10B**). The analyzed data for beat frequency and interspike interval will be saved in the form of ASCII (text) format.

NOTE: To analyze different conditions (such as baseline and drug response), analysis must be run separately for each condition.

12.8. Click the **Play and Record** button on the top tab bar to start the analysis.

12.9. To export the data for other applications, select the boxes for **Save beat per minute** and **Save interspike interval** (**Figure 10B**). Enter the desired file name in the **File name modifier** box (**Figure 10B**) and click **Save** to save the analyzed data in ASCII text format in the selected folder.

REPRESENTATIVE RESULTS:

After allowing the tissue to acclimate in the dish for 15 min, 10 one-min traces are recorded. Our current protocol records activity for over an hour, but we have recorded stable firing patterns for ≥4 h in unpublished data not shown here. If an experimental preparation is good for data collection, each recording channel should exhibit consistent and evenly spaced recurring waveforms (i.e., spikes) of uniform shape for a given channel (**Figure 11D**). These waveforms correspond to individual heart beats that reflect intrinsic cardiac pacemaking activity. The interspike intervals should be the same for every channel even if they may not be perfectly aligned across channels due to small differences in their location relative to the initiation site of depolarization (**Figure 8**). Although the shape of the waveforms for a given channel should be consistent, the shape of the waveforms will vary across channels depending on the location of the electrode in the tissue (**Figure 8**). The degree of contact of the tissue with the electrode may also influence waveform characteristics, such as the amplitude. However, the amplitude maxima should be at least 0.5 mV for the majority of channels if the preparation is satisfactory. From the 10 recorded traces, the three consecutive channels that best meet the quality criteria described above were chosen for further analysis described below. **Figure 10A** shows a sample of stable beat frequency (top panel) and interspike interval (middle panel) for three consecutive traces. Tissue that does not meet these criteria should not be recorded as there is likely tissue damage that will hinder accurate data collection. **Figure 11** shows examples of bad extracted spike patterns which are either absent (**A**), influenced by noise (**B**), or unstable (**C**).

The sample data displayed in the figures was collected from a 45-day old male wildtype Black

Swiss (Tac:N:NIHS-BC) mouse. The analysis procedure depicted in **Figure 9** and **Figure 10** was used to extract the intrinsic firing rate and display baseline spikes that can be seen in **Figure 12A**. The firing rate is the average rate across 60,000 ms from each of the three traces, but the spike pattern in **Figure 12A** shows 5 s of representative spiking from a single trace. Using automated analysis software, the intrinsic firing rate (i.e., beat frequency) of the selected three traces across all 64 channels was found to be approximately 320 bpm in our sample data (**Figure 12A**). In general, we observe a range of values of about 290-340 bpm in our recordings for wildtype mice. The firing rate can also be used as a secondary method to assess preparation quality. Rates that are either unstable or significantly lower than 300 bpm are less likely to be good for analysis. These values are comparable to both isolated heart and single cell recordings which report intrinsic heart rates in the range of approximately 300-500 bpm[25,48,49]. Therefore, the MEA recording technique is capable of generating reliable and accurate measures of intrinsic heart rate.

An advantage of the MEA system is that it allows easy application of drug agents to test pharmacological effects. In the sample experiment, we tested the effects of 1 mM 4-AP on firing rate, which should slow SAN activity since blockade of voltage-gated K^+ channels is known to impair action potential repolarization in SA cells[24,50]. **Figure 12B** shows that the introduction of 4-AP increased the interspike intervals as expected. This prolonged spike interval corresponded to a decrease in the beat frequency from 320 bpm to 210 bpm. This firing rate following 4-AP administration is similar to a previous study that examined the effects of 4-AP on SAN firing rate using single electrode recordings of isolated tissue. That study measured a firing rate of approximately 190 bpm in the presence of 4-AP[50]. Thus, the MEA system can be used as a convenient and valuable tool for testing pharmacological effects of drug interventions on intrinsic cardiac function.

FIGURE AND TABLE LEGENDS:

Figure 1: Coating the microelectrode array (MEA) prior to use. (**A**) The MEA is composed of a small plastic dish with a grid array of 64 microelectrodes in the center (as shown in the panel **A1**) and four reference electrodes around the periphery in a square pattern. (**B**) Addition of 1 mL of PEI buffer to coat the MEA. (**C**) Covering the MEA dish with thermoplastic film for incubation overnight at room temperature. (**D**) Aspirating the PEI buffer from the MEA dish, which is followed by at least four rinses with distilled water. (**E**) Storing the coated MEA probe under ultrapure water to prevent it from drying out.

Figure 2: Tools used for sinoatrial node (SAN) dissection. The following tools are used during the dissection part of the protocol: (i) Petri dish with silicone elastomer and small dissection pins; (ii) Plastic transfer pipette; (iii) Castroviejo scissor, size 4”; (iv) Surgical scissors (straight) for cutting procedures; (v) Dumont #2 Laminectomy forceps; (vi) Dumont #55 forceps; (vii) Extra fine Graefe forceps; (viii) Hemostats (curved).

Figure 3: Removal of the heart. (**A**) Transverse incision in the skin just beneath the bottom of the rib cage from about the left costal arch to the right costal arch. (**B**) Peritoneal incision. (**C,D**) Incision of the diaphragm along the thorax to expose the thoracic cavity. (**E**) Removal of the heart

following excision of the lungs.

Figure 4: Dissection of the sinoatrial (SAN) node. (**A**) The appearance of the heart in the Petri dish following removal from the body. (**B**) Insertion of the syringe needle through the inferior vena cava (IVC) and superior vena cava (SVC) of the right atrium. The pin in the apex of the heart is also shown. (**C**) Excision of the apex (i.e., the bottom half) of the heart to release the blood. The pins in the atrial appendages are also shown. (**D**) The final appearance of the SAN region of the right atrium at the end of dissection. The boxed region corresponds to the approximate location of the SAN. The SAN artery can also be faintly seen coursing through the SAN in a vertical orientation. The Abbreviations: AO, aorta; CT, crista terminalis; IVC, inferior vena cava; LA, left atrium; RA, right atrium; RAA, right atrial appendage; SAN, sinoatrial node; SVC, superior vena cava.

Figure 5: Schematic of the microelectrode array (MEA) recording system setup. The following components comprise the system: (**A**) gas cylinder (carbogen: 95% O_2/ 5% CO_2); (**B**) conical flask with distilled water to humidify the gas; (**C**) recording Tyrode's solution bottle that provides inflow to the MEA dish; (**D**) peristaltic pump to pump solution to and from the MEA dish; (**E**) temperature regulator; (**F**) MEA connector plate which receives signals from the MEA dish; (**G**) amplifier; (**H**) computer; (**I**) collection bottle for used waste solution from the MEA dish.

Figure 6: Positioning of the SA nodal tissue on MEA. (**A**) Tools used in positioning the tissue: (i) Mesh with 1.5-mm grid size, (ii) harp anchor, (iii) bone forceps, (iv) paint brush. (**B**) Positioning of the tissue on the MEA. The yellow box indicates the approximate area of the sinoatrial node region under the mesh and anchor in the MEA dish. (**C**) Arrangement of the MEA dish with enclosed tissue on the connector plate for field potential recording: (i) inlet for the recording solution; (ii) inlet for gas (carbogen); (iii) outlet for the solution; (iv) microelectrode connector plate; (v) perfusion cap; (vi) reference electrode ring attached to the cap; (vii) tape to hold the cap.

Figure 7: Setting the data acquisition protocol in the software. (**A**) An example of recording template showing arrangement of all 64 channels. (**B**) An example of the software input properties for the recording conditions. (**C**) An example of the **Annotations** menu showing how to **Add New Phase** during the recording, such as for measuring drug effects.

Figure 8: Different regions of the tissues showing different activity waveforms. Example screen shot showing waveforms with different shapes and amplitudes in different channels. However, all channels show identical interspike intervals and firing frequencies. The channels within the red box correspond approximately to the electrodes placed within the SAN region of the tissue.

Figure 9: Beat frequency analysis template. Example template showing arrangement of all 64 channels in beat frequency analysis template. The **Replay Raw Data File** inset shows an example of the input properties of the analysis window. In this example, traces 5 to 7 have been selected for analysis and the duration of analysis for each trace has been designated as 60,000 ms.

Figure 10: Defining analysis parameters for spike extraction. (**A**) Representative analysis template results for 3 selected traces of a single channel. The top panel displays beat frequency for the three selected traces (three defined groupings of data points), and each point represents a 10-s average for beat frequency during the specific trace. The middle panel displays inter-spike interval for the three selected traces (three defined groupings of data points), and each data point represents the inter-spike interval between two consecutive spikes. The lower left panel shows selected representative extracted spikes for the last 5 s of the third trace, whereas the lower right panel shows an extracted waveform derived from the 5-s group of extracted spikes in the lower left panel. (**B**) Expanded view of the analysis window showing parameters used in the analysis of beating frequency for the 3 traces.

Figure 11: Representative figure showing good versus bad data extraction for a particular channel. Bad data extraction: (**A**) Absence of extracted spikes; (**B**) Extracted spikes with noise signals; (**C**) Unstable extracted spikes. (**D**) Good data showing stable extracted spikes without noise signals.

Figure 12: Recordings at baseline and after administration of 1mM 4-Aminopyridine (4-AP). (**A**) Baseline recording from a single microelectrode shows waveforms with a stable firing frequency of 320 bpm in a WT heart. (**B**) Following administration of 4-AP, the firing frequency slows to a stable rate of 210 bpm.

DISCUSSION:

Practicing and mastering the SAN dissection process is imperative since the tissue is fragile and healthy tissue is necessary for a successful recording. During the SAN dissection, correct orientation is essential to obtain the proper region of tissue. However, the original orientation of the heart can be easily lost during the dissection process, which complicates this endeavor. Therefore, to ensure the proper left-right orientation, the atria should be visually inspected. Typically, the right atrium tends to be more transparent, whereas the left atrium is usually darker and more red in color[25,48]. Furthermore, it is essential not to stretch the SAN tissue while working with it or mounting it onto the electrode grid, as the tissue is easily mechanically damaged[51]. A tip to verify healthy and properly dissected SAN tissue is to examine it in Complete Tyrode's solution under the microscope to verify that the tissue is beating. Once the technique is mastered, at least 90% of tissue preparations should be good for recording.

Several considerations can improve the likelihood of successful recordings and subsequent data analysis. To ensure the best recordings, solutions should be carefully prepared and tested on practice mouse samples prior to experimental recordings. We worked extensively to adapt and modify the recording solution to optimize the health of the SAN tissue. Additionally, ensure that the gas used for the recording is carbogen (i.e., 95% O_2/5% CO_2). Single cell recordings often use pure oxygen due to the specific chemical composition of the Tyrode's solution used for that application, but the solution used for recording on the MEA requires carbogen in order to maintain a stable pH. Using pure oxygen with the Tyrode's solution for the MEA recordings will cause fluctuations in the pH which can lead to rapid deterioration of the tissue. Assessing the amplitude maxima in the channels as previously described will help determine if the tissue is of

good recording quality. Finally, to aid analysis after the recording, taking an image of the mounted SAN tissue on the MEA electrode array after the recording is finished is very helpful. The tissue can shift slightly during the initial set up of the MEA, and this provides the most accurate assessment of electrode placement for analysis.

We propose MEA recordings as a thorough and accurate way to characterize SAN firing rate. An advantage of the MEA technique is that it allows the experimenter to capture firing rates on par with single cell recordings without the need to have extensive electrophysiological expertise. The MEA technique also has the advantage of eliminating the potential confounding influences of neurohumoral and mechano-electric mechanisms, which are inherent in isolated heart recordings and *in vivo* autonomic blockade measurements[21]. Ventricular contraction and respiration are the main mechano-electric influences that could alter SAN firing, but they are eliminated in our tissue preparation [52,53]. While our technique eliminates most of the autonomic influences on the SAN, a limited number of remaining ICNS projections in the right atria could potentially impact SAN firing, a theoretical limitation which should be kept in mind during the interpretation of results[5,6,22,23]. Another advantage of the MEA technique described here is that it can be adapted for many other types of cardiac studies. For example, although this protocol demonstrated the effects of 4-AP on SAN activity, future studies could look at an almost limitless number of pharmacological agents, as well as the effects of gene mutations on SAN intrinsic firing. For example, ivabradine, a specific blocker of the SAN-specific Hcn4 channel, could be used to study funny current contributions to the firing rate[54]. The MEA system can also be used to measure cardiac function in other regions of the heart, allowing for detailed, region-specific characterization. However, recording from other heart regions would require different dissection approaches and the possibility of thin tissue sectioning before recording. One potentially significant limitation of this technique is the high cost of purchasing an MEA system which can be prohibitive. Several MEA systems are available on the market with similar characteristics and functionality, but the high cost remains the same. However, once the initial equipment and software is acquired, the cost to maintain and use the MEA system is fairly low. Another limitation is that the MEA system only allows recording of extracellular field potentials which are not conducive to precise comparisons of action potential characteristics (e.g., amplitude and shape) between preparations such as can be attained with single cell intracellular recordings. In summary, this protocol provides an efficient workflow to measure and analyze intrinsic cardiac firing rates in mouse SAN tissue with the ability to study the effects of pharmacological intervention on firing rate in a highly specific manner.

ACKNOWLEDGMENTS:
This work was funded by the National Institutes of Health, grant numbers R01NS100954 and R01NS099188.

DISCLOSURES:
The authors have nothing to disclose.

REFERENCES:
1. Marionneau, C. et al. Specific pattern of ionic channel gene expression associated with

pacemaker activity in the mouse heart. *Journal of Physiology*. **562** (1), 223–234 (2005).
2. Josea, A. D., Collison, D. The normal range and determinants of the intrinsic heart rate in man. *Cardiovascular Research*. (4), 160–167 (1970).
3. Peters, C. H., Sharpe, E. J., Proenza, C. Annual Review of Physiology Cardiac Pacemaker Activity and Aging. *Annual Review of Physiology*. **82**, 21–43 (2019).
4. Keith, A., Flack, M. The form and nature of the muscular connections between the primary divisions of the vertebrate heart. *Journal of Anatomy and Physiology*. **41** (3), 172–189 (1907).
5. Wake, E., Brack, K. Characterization of the intrinsic cardiac nervous system. *Autonomic Neuroscience*. **199** (2016).
6. Fedele, L., Brand, T. The intrinsic cardiac nervous system and its role in cardiac pacemaking and conduction. *Journal of Cardiovascular Development and Disease*. **7** (4), 1–33 (2020).
7. Mangrum, J. M., DiMarco, J. P. The evaluation and management of bradycardia. *New England Journal of Medicine*. **342** (10), 703–709 (2000).
8. Adan, V., Crown, L. A. Diagnosis and treatment of Sick Sinus Syndrome. *American Family Physician*. **67** (8), 1725–1732 (2003).
9. Semelka, M., Gera, J., Usman, S. Sick Sinus Syndrome: A Review. *American Family Physician*. **87** (10), 691–696 (2013).
10. Zaragoza, M. V. et al. Exome sequencing identifies a novel LMNA splice-site mutation and multigenic heterozygosity of potential modifiers in a family with Sick Sinus Syndrome, dilated cardiomyopathy, and sudden cardiac death. *PLoS ONE*. **11** (5), e0155421 (2016).
11. Brugada, J., Campuzano, O., Arbelo, E., Sarquella-Brugada, G., Brugada, R. Present status of Brugada Syndrome: JACC State-of-the-Art Review. *Journal of the American College of Cardiology*. **72** (9), 1046–1059 (2018).
12. Rollin, A. et al. Prevalence, characteristics, and prognosis role of type 1 ST elevation in the peripheral ECG leads in patients with Brugada syndrome. *Heart Rhythm*. **10** (7), 1012–1018 (2013).
13. Patel, N., Majeed, F., Sule, A. A. Seizure triggered by Sick Sinus Syndrome. *BMJ case reports.* **4**, bcr2017222011. (2017).
14. Knecht, S. et al. Impact of pharmacological autonomic blockade on complex fractionated atrial electrograms. *Journal of Cardiovascular Electrophysiology*. **21** (7), 766–772 (2010).
15. Saba, S., London, B., Ganz, L. Autonomic blockade unmasks maturational differences in rate-dependent atrioventricular nodal conduction and facilitation in the mouse. *Journal of Cardiovascular Electrophysiology*. **14** (2), 191–195 (2003).
16. Shusterman, V. et al. Strain-specific patterns of autonomic nervous system activity and heart failure susceptibility in mice. *American Journal of Physiology - Heart and Circulatory Physiology*. **282** (6), 51–56 (2002).
17. Tse, G., Tse, V., Yeo, J. M., Sun, B. Atrial anti-arrhythmic effects of heptanol in Langendorff-perfused mouse hearts. *PLoS ONE*. **11** (2), e0148858 (2016).
18. Tse, G. et al. Quantification of beat-to-beat variability of action potential durations in Langendorff-perfused mouse hearts. *Frontiers in Physiology*. **9** (1578), e01578 (2018).
19. Avula, U. M. R. et al. Heterogeneity of the action potential duration is required for sustained atrial fibrillation. *JCI Insight*. **5** (11), e128765 (2019).
20. Jungen, C. et al. Impact of intracardiac neurons on cardiac electrophysiology and

arrhythmogenesis in an ex vivo Langendorff system. *Journal of Visualized Experiments*. (135), e57617 (2018).
21. Quinn, A. T., Kohl, P. Cardiac mechano-electric coupling: Acute effects of mechanical stimulation on heart rate and rhythm. *Physiological Reviews*. **101** (1), 37–92 (2021).
22. Ripplinger, C. M., Noujaim, S. F., Linz, D. The nervous heart. *Progress in Biophysics and Molecular Biology*. **120** (1–3), 199–209 (2016).
23. Pauza, D. H., Pauziene, N., Pakeltyte, G., Stropus, R. Comparative quantitative study of the intrinsic cardiac ganglia and neurons in the rat, guinea pig, dog and human as revealed by histochemical staining for acetylcholinesterase. *Annals of Anatomy*. **184**, 125–136 (2002).
24. Golovko, V., Gonotkov, M., Lebedeva, E. Effects of 4-aminopyridine on action potentials generation in mouse sinoauricular node strips. *Physiological Reports*. **3** (7), e12447 (2015).
25. Sharpe, E. J., St. Clair, J. R., Proenza, C. Methods for the isolation, culture, and functional characterization of sinoatrial node myocytes from adult mice. *Journal of Visualized Experiments*. (116), e54555 (2016).
26. Doi, M., Ogawa, E., Arai, T. Effect of a photosensitization reaction performed during the first 3 min after exposure of rat myocardial cells to talaporfin sodium in vitro. *Lasers in Medical Science*. **32** (8), 1873–1878 (2017).
27. Takanari, H. et al. A new in vitro co-culture model using magnetic force-based nanotechnology. *Journal of Cellular Physiology*. **231** (10), 2249–2256 (2016).
28. Nakashima, T. et al. Rapid electrical stimulation causes alterations in cardiac intercellular junction proteins of cardiomyocytes. *American Journal of Physiology-Heart and Circulatory Physiology*. **306** (9), H1324–H1333 (2014).
29. Suzuki, S. et al. Effects of aldosterone on Cx43 gap junction expression in neonatal rat cultured cardiomyocytes. *Circulation Journal*. **73** (8), eCJ-08-1065 (2009).
30. Horiba, M. et al. T-type Ca2+ channel blockers prevent cardiac cell hypertrophy through an inhibition of calcineurin–NFAT3 activation as well as L-type Ca2+ channel blockers. *Life Sciences*. **82** (11–12), 554–560 (2008).
31. Inoue, N. et al. Rapid electrical stimulation of contraction modulates gap junction protein in neonatal rat cultured cardiomyocytes: involvement of mitogen-activated protein kinases and effects of angiotensin II receptor agonist. *Journal of the American College of Cardiology*. **44** (4), 914–922 (2004).
32. Aalders, J. et al. Effects of fibrillin mutations on the behavior of heart muscle cells in Marfan syndrome. *Scientific Reports*. **10** (16756) (2020).
33. Matsuura, K. et al. Creation of mouse embryonic stem cell-derived cardiac cell sheets. *Biomaterials*. **32** (30), 7355–7362 (2011).
34. Fujita, H., Shimizu, K., Nagamori, E. Application of a cell sheet-polymer film complex with temperature sensitivity for increased mechanical strength and cell alignment capability. *Biotechnology and Bioengineering*. **103** (2), 370–377 (2009).
35. Baba, S. et al. Generation of cardiac and endothelial cells from neonatal mouse testis-derived multipotent germline stem cells. *Stem Cells*. **25** (6), 1375–1383 (2007).
36. Baba, S. et al. Flk1+ cardiac stem/progenitor cells derived from embryonic stem cells improve cardiac function in a dilated cardiomyopathy mouse model. *Cardiovascular Research*. **76** (1), 119–131 (2007).
37. Shimizu, K. et al. Construction of multi-layered cardiomyocyte sheets using magnetite

nanoparticles and magnetic force. *Biotechnology and Bioengineering*. **96** (4), 803–809 (2007).
38. Haraguchi, Y., Shimizu, T., Yamato, M., Kikuchi, A., Okano, T. Electrical coupling of cardiomyocyte sheets occurs rapidly via functional gap junction formation. *Biomaterials*. **27** (27), 4765–4774 (2006).
39. Miyagawa, S. et al. Tissue cardiomyoplasty using bioengineered contractile cardiomyocyte sheets to repair damaged myocardium: Their integration with recipient myocardium. *Transplantation*. **80** (11), 1586–1595 (2005).
40. Watts, M. et al. Decreased bioavailability of hydrogen sulfide links vascular endothelium and atrial remodeling in atrial fibrillation. *Redox Biology*. **38**, 101817 (2021).
41. Feng, Y., Cao, H., Zhang, Y. Prediction model of sinoatrial node field potential using high order partial least squares. *Bio-Medical Materials and Engineering*. **26**, S1805–S1811 (2015).
42. Feng, Y., Cao, H., Wang, Y., Zhang, Y. Fuzzy linguistic prediction model for sinoatrial node field potential analysis in acute hyperglycemia environment. *Bio-Medical Materials and Engineering*. **26** (Suppl 1), S881-887 (2015).
43. Suzuki, K., Matsumoto, A., Nishida, H., Reien, Y., Maruyama, H., Nakaya, H. Termination of aconitine-induced atrial fibrillation by the KACh-channel blocker tertiapin: underlying electrophysiological mechanism. *Journal of Pharmacological Sciences*. **125** (4), 406–414 (2014).
44. Chang, S.-L. et al. Heart failure enhances arrhythmogenesis in pulmonary veins. *Clinical and Experimental Pharmacology and Physiology*. **38** (10), 666–674 (2011).
45. Wang, Y.-J. et al. Time-dependent block of ultrarapid-delayed rectifier K+ currents by aconitine, a potent cardiotoxin, in heart-derived H9c2 myoblasts and in neonatal rat ventricular myocytes. *Toxicological Sciences*. **106** (2), 454–463 (2008).
46. Lai, Y.-J., Huang, E. Y.-K., Yeh, H.-I., Chen, Y.-L., Lin, J. J.-C., Lin, C.-I. On the mechanisms of arrhythmias in the myocardium of mXinα-deficient murine left atrial-pulmonary veins. *Life Sciences*. **83** (7–8), 272–283 (2008).
47. Gustafson-Wagner, E. A. et al. Loss of mXinα, an intercalated disk protein, results in cardiac hypertrophy and cardiomyopathy with conduction defects. *American Journal of Physiology-Heart and Circulatory Physiology*. **293** (5), H2680–H2692 (2007).
48. Clark, R. B. et al. A rapidly activating delayed rectifier K+ current regulates pacemaker activity in adult mouse sinoatrial node cells. *American Journal of Physiology-Heart and Circulatory Physiology*. **286**, H1757-1766 (2004).
49. Bell, R. M., Mocanu, M. M., Yellon, D. M. Retrograde heart perfusion: The Langendorff technique of isolated heart perfusion. *Journal of Molecular and Cellular Cardiology*. **50** (6), 940–950 (2011).
50. Nikmaram, M. R. et al. Characterization of the effects of Ryanodine, TTX, E-4031 and 4-AP on the sinoatrial and atrioventricular nodes. *Progress in Biophysics and Molecular Biology*. **96** (1–3), 452–464 (2008).
51. Fenske, S. et al. Comprehensive multilevel in vivo and in vitro analysis of heart rate fluctuations in mice by ECG telemetry and electrophysiology. *Nature Protocols*. **11** (1), 61–86 (2016).
52. Masé, M., Glass, L., Ravelli, F. A model for mechano-electrical feedback effects on atrial flutter interval variability. *Bulletin of Mathematical Biology*. **70** (5), 1326–1347 (2008).
53. Franz, M. R., Bode, F. Mechano-electrical feedback underlying arrhythmias: The atrial fibrillation case. *Progress in Biophysics and Molecular Biology*. **82** (1–3), 163–174 (2003).

54. Bucchi, A., Tognati, A., Milanesi, R., Baruscotti, M., DiFrancesco, D. Properties of ivabradine-induced block of HCN1 and HCN4 pacemaker channels. *Journal of Physiology*. **572** (2), 335–346 (2006).

Fig 1

Figure 1

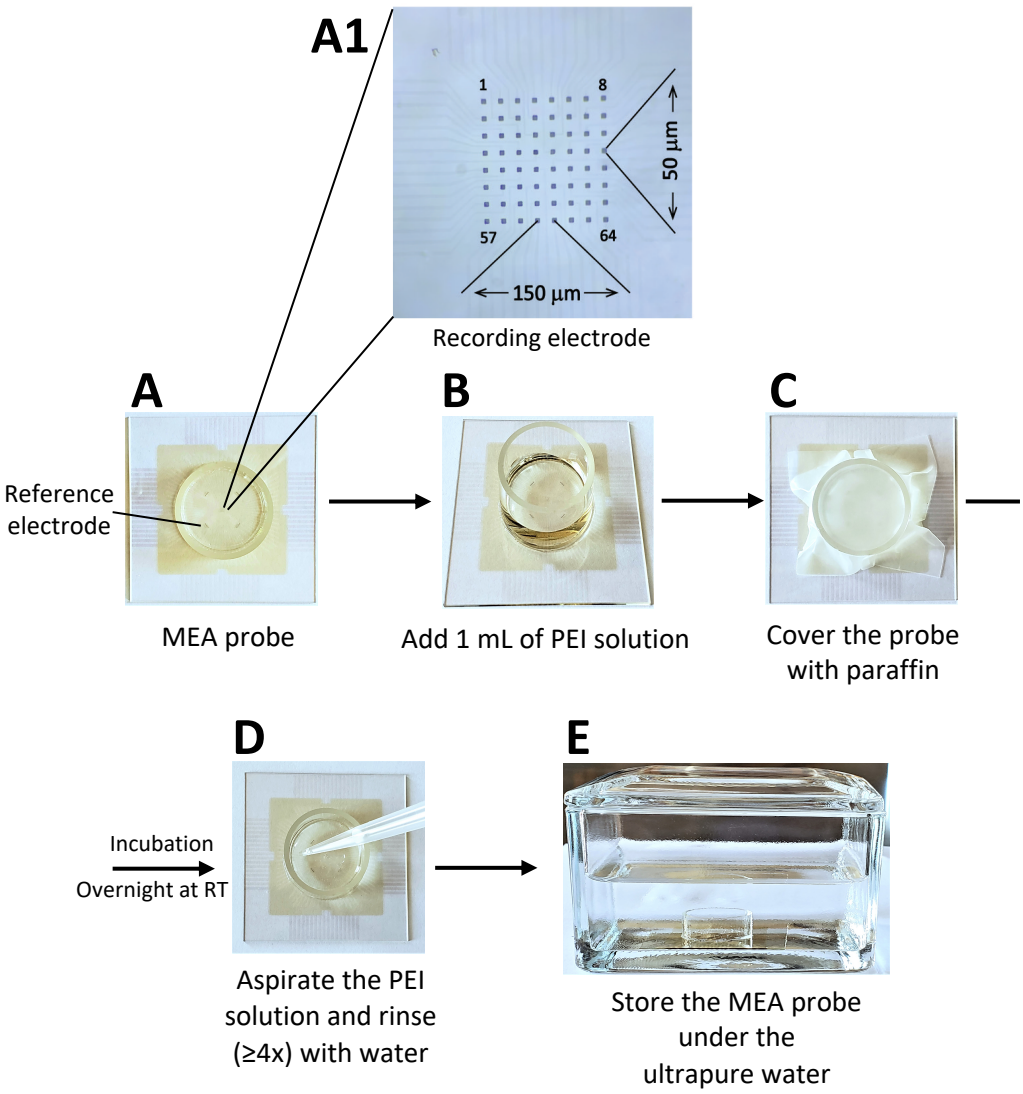

Fig 2

Figure 2

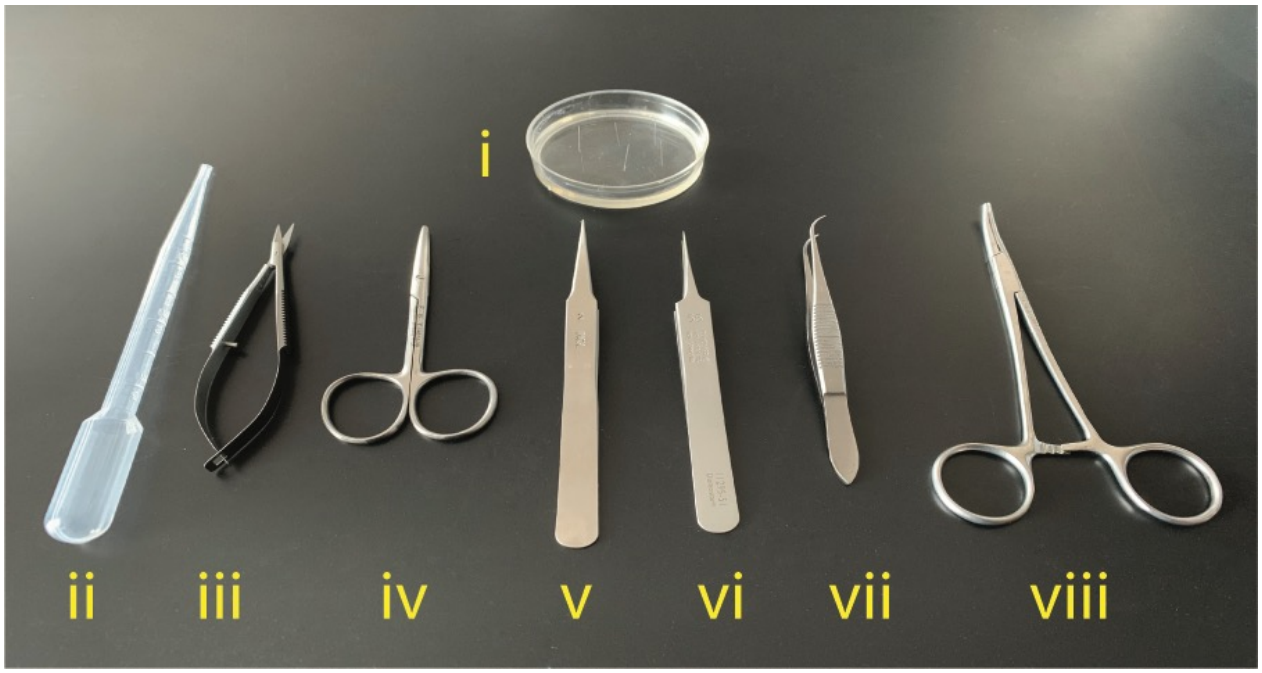

Fig 3 **Figure 3**

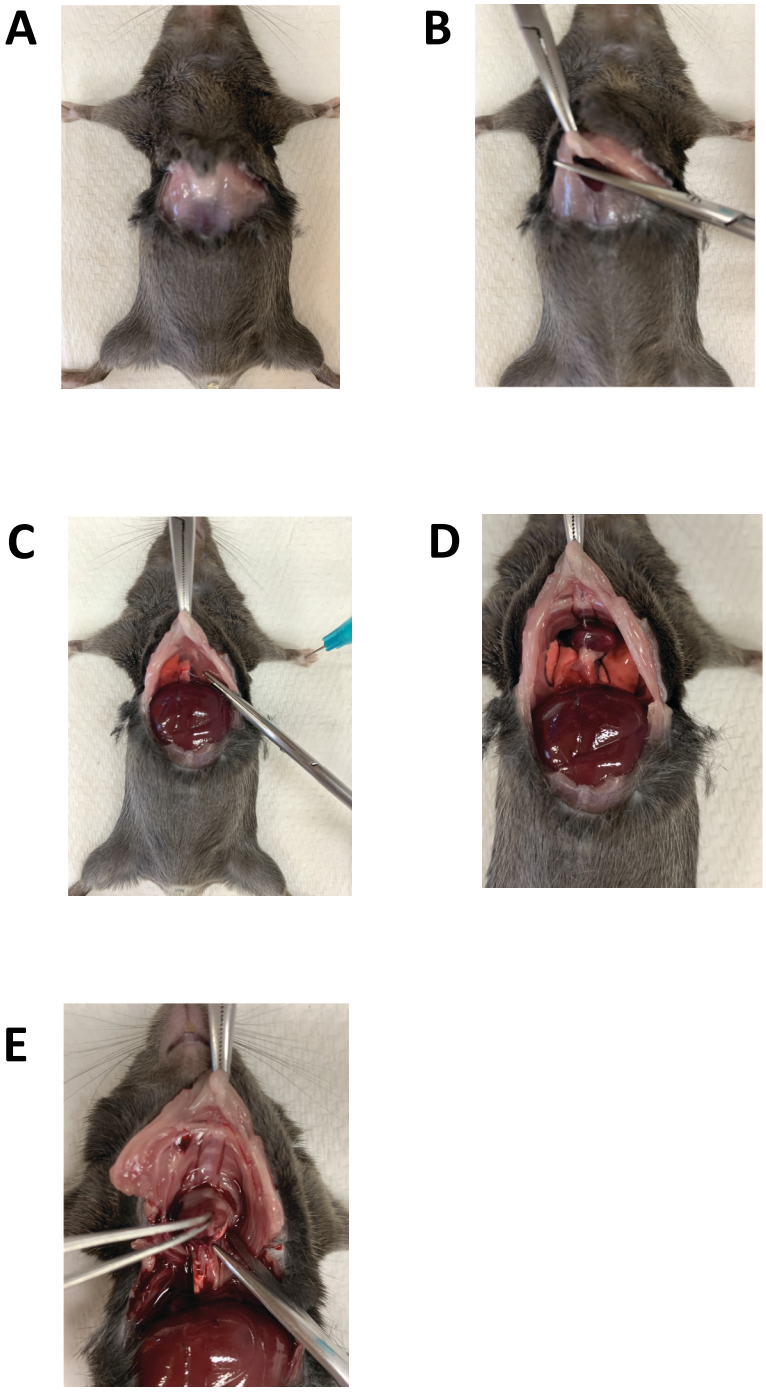

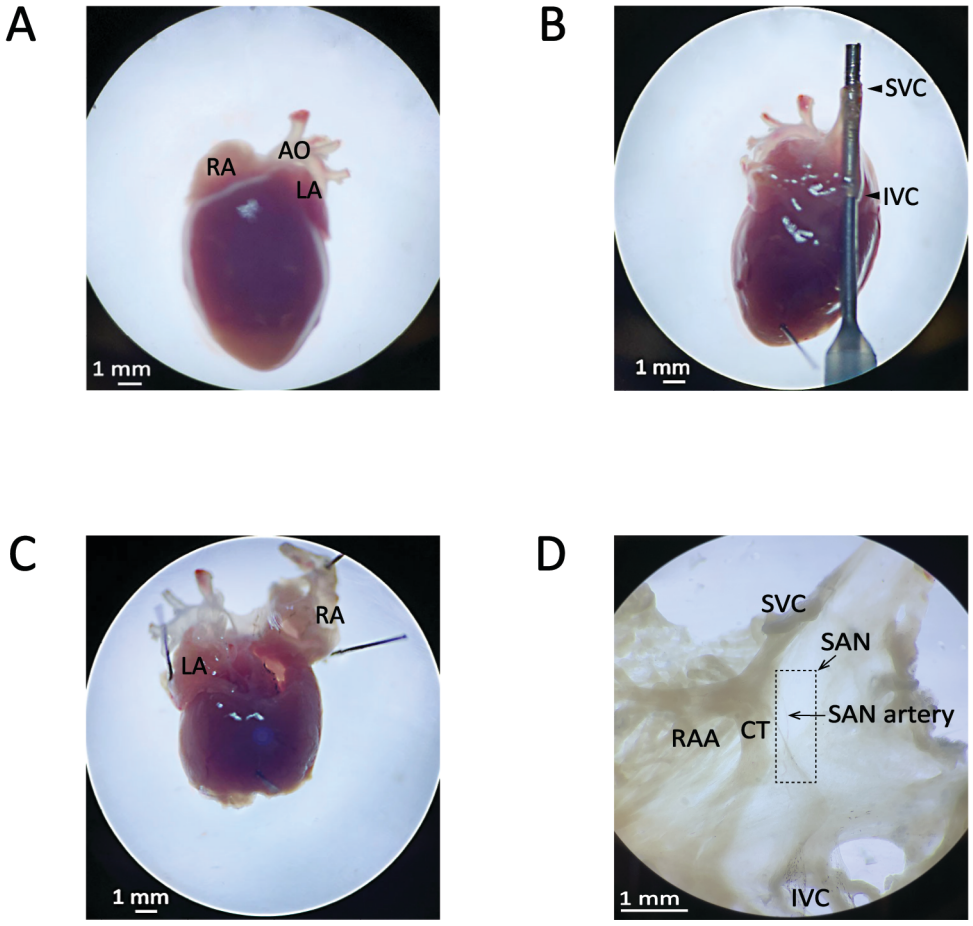

Fig 5

Figure 5

Click here to access/download;Figure;Figure 5.pdf

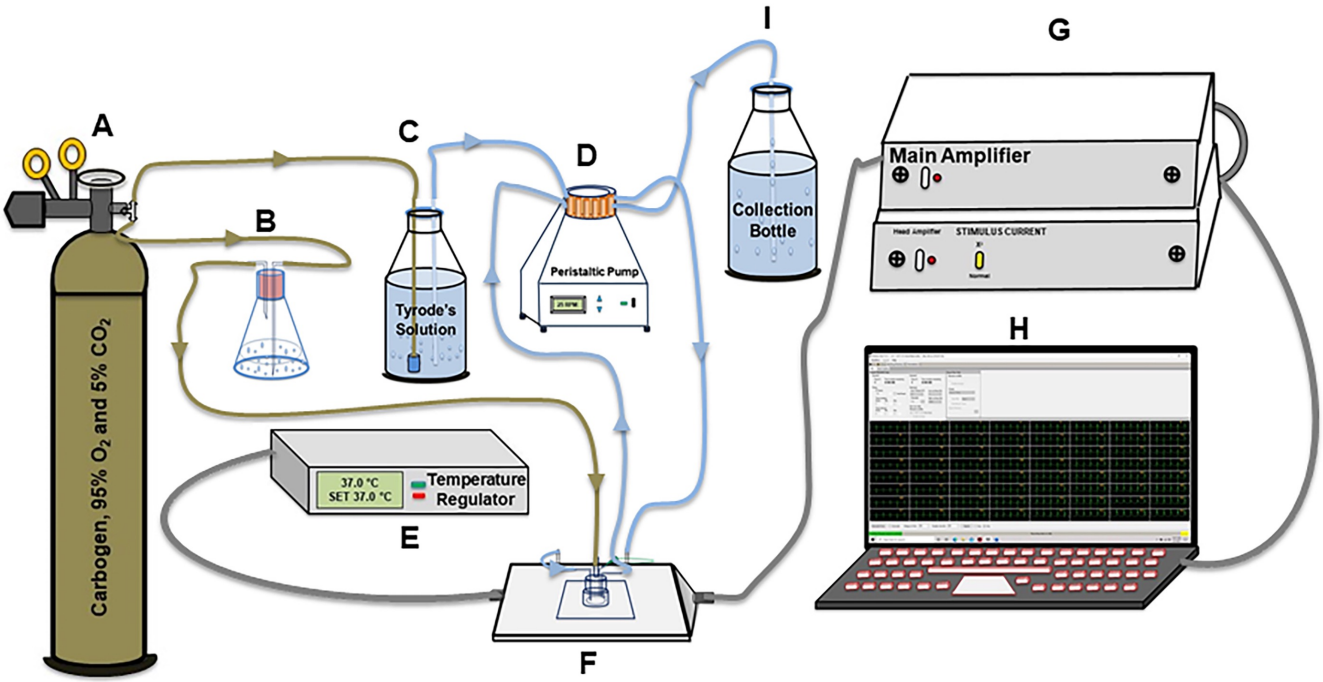

Fig 6

Figure 6

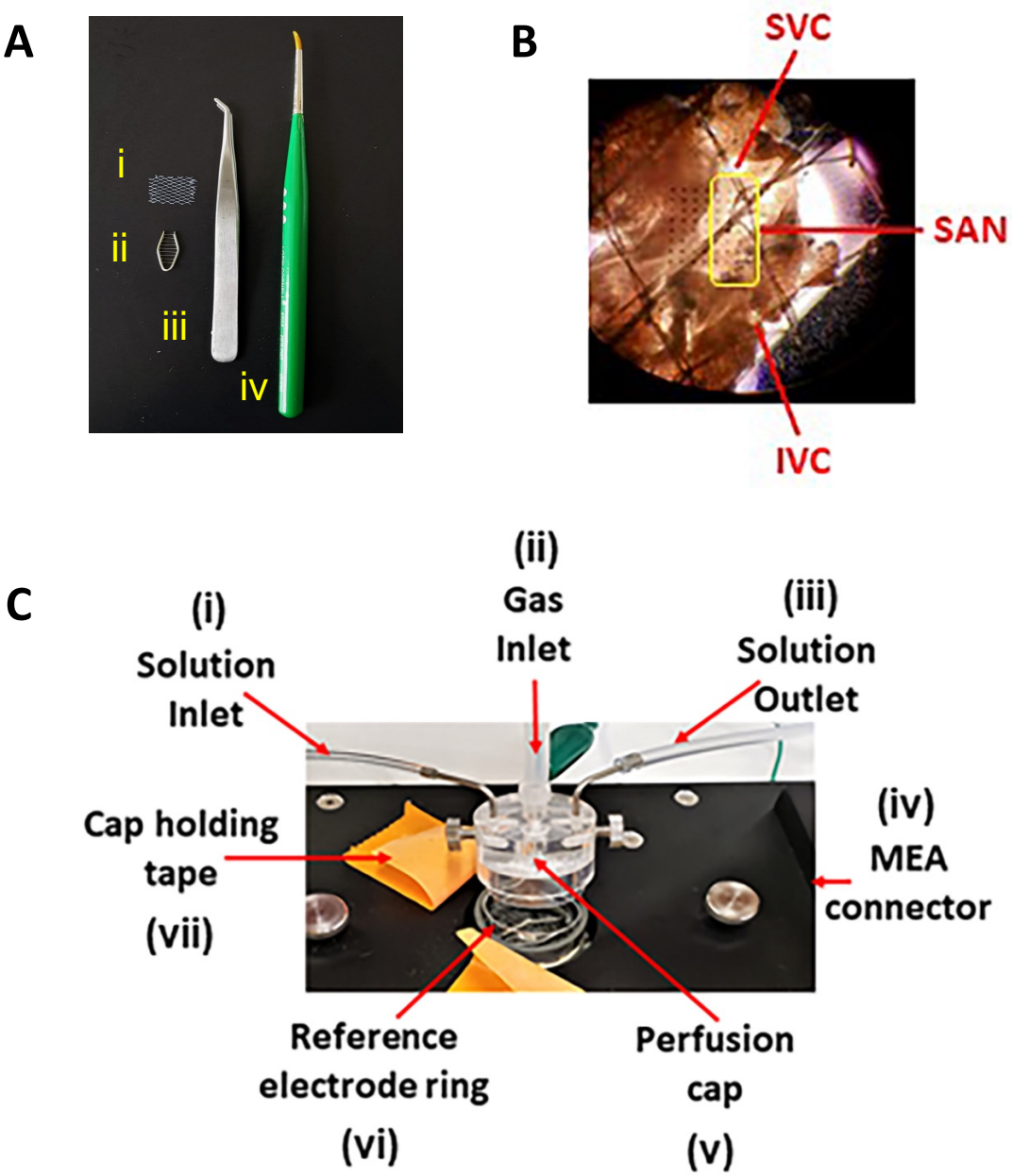

Fig 7

Figure 7

Click here to access/download;Figure;Figure 7.pdf

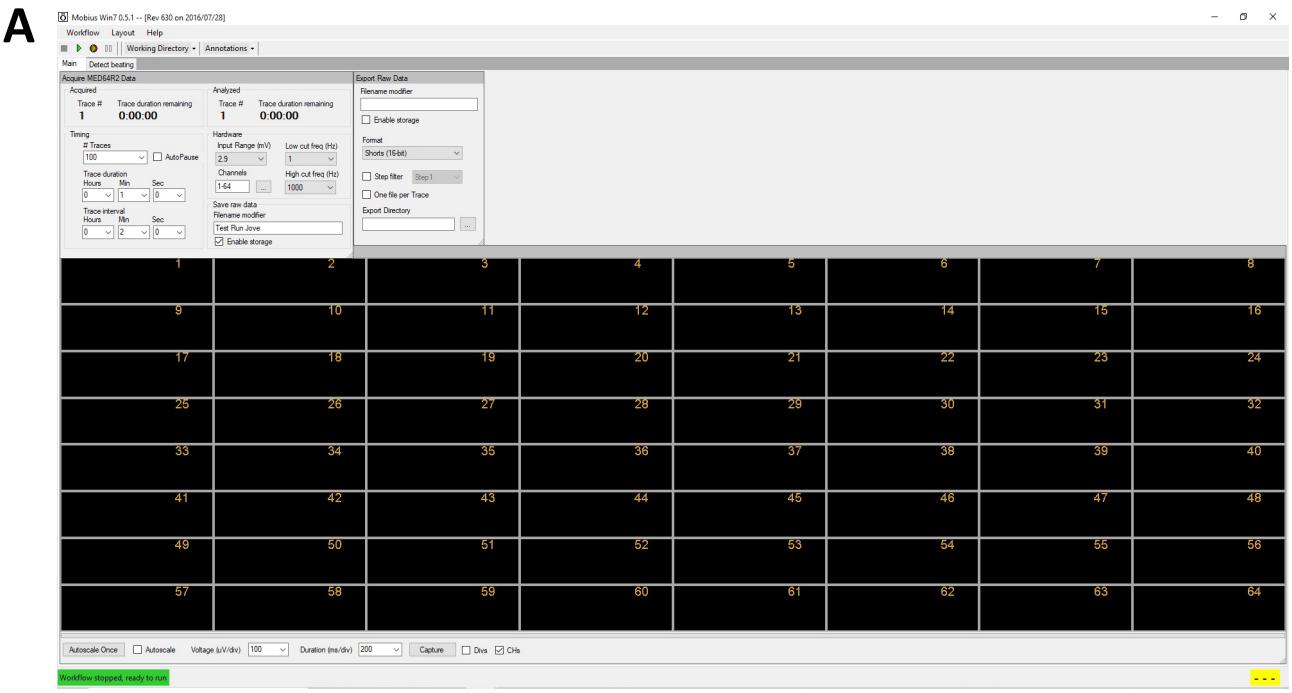

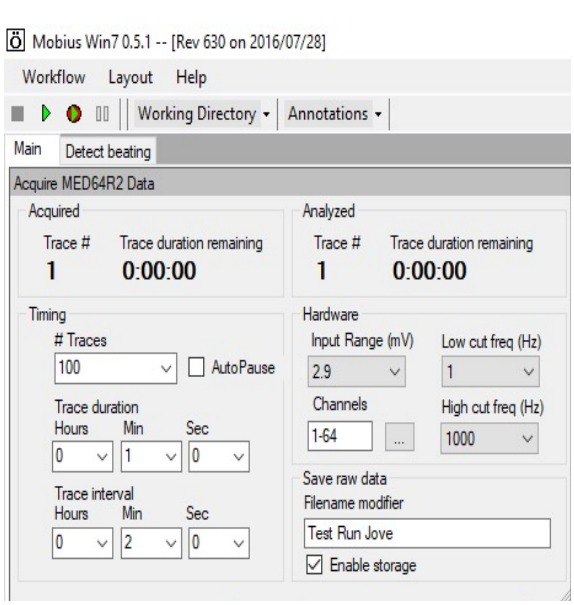

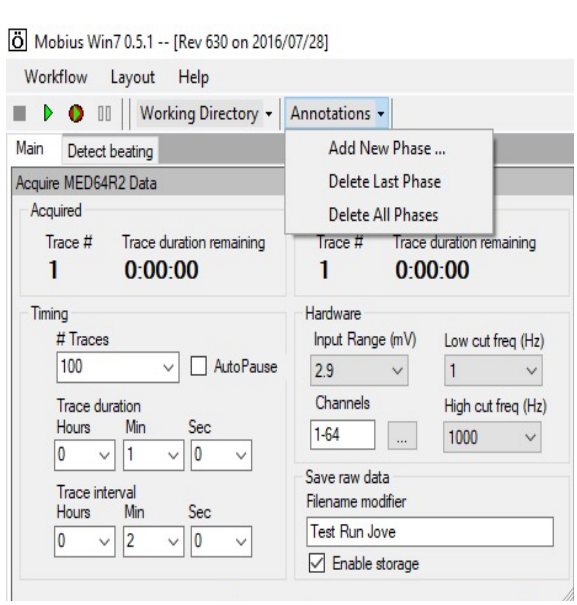

Fig 8 **Figure 8**

Click here to access/download;Figure;Figure 8.pdf

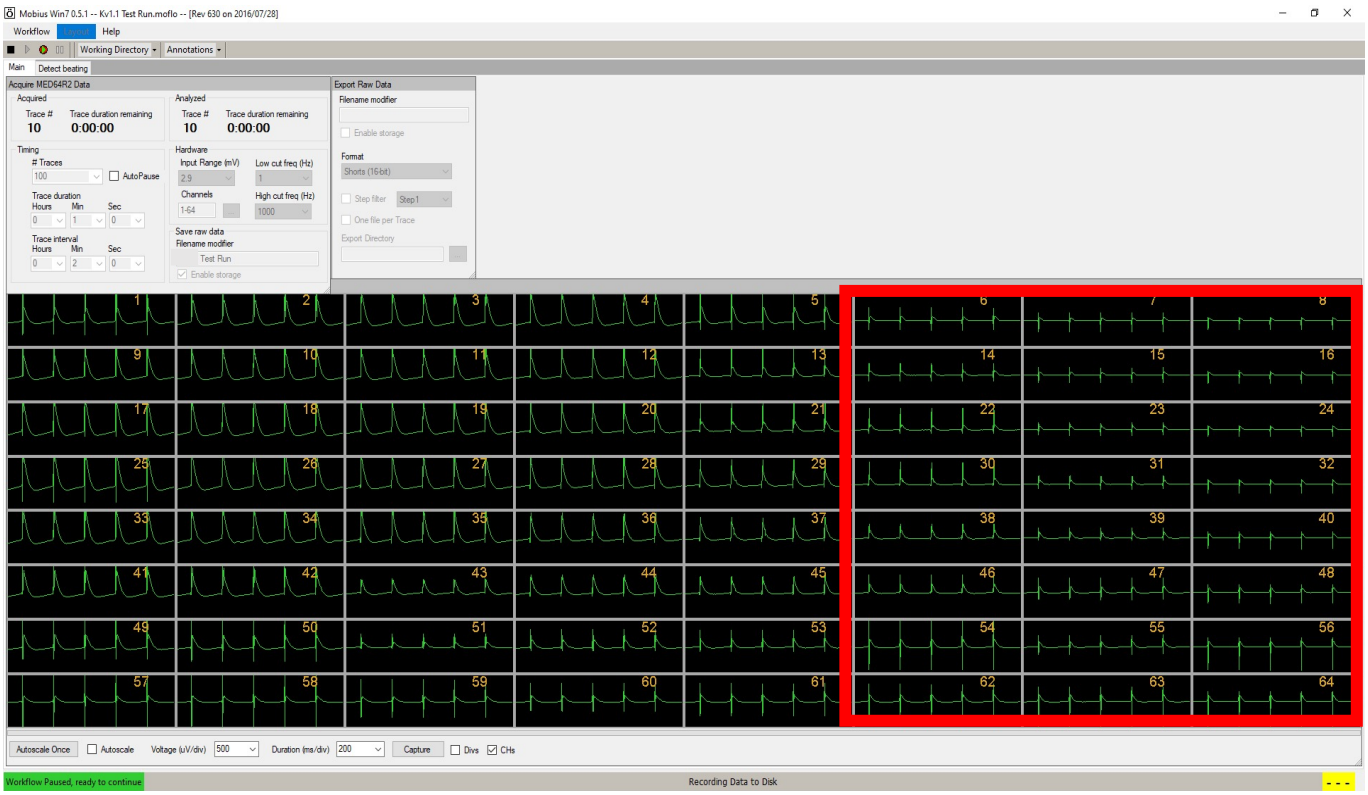

Fig 9

Figure 9

Click here to access/download;Figure;Figure 9.pdf

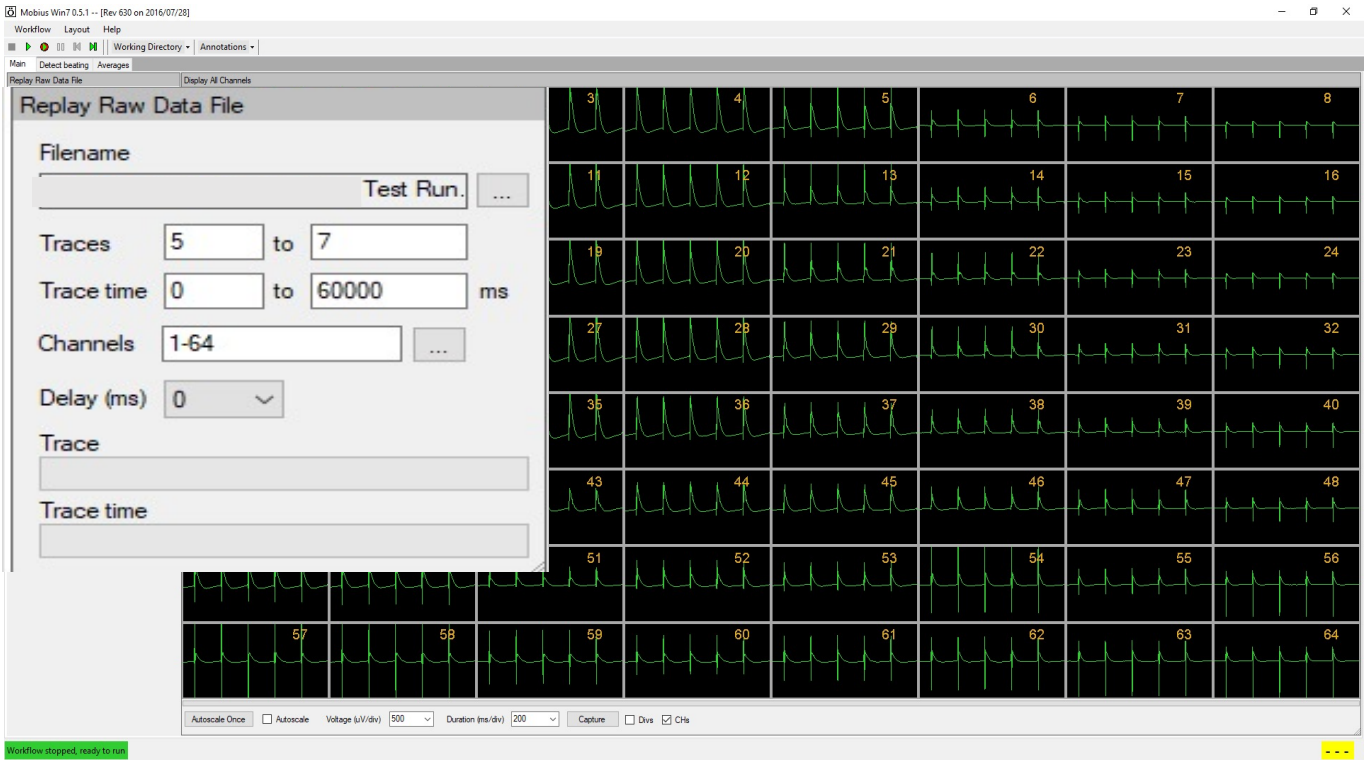

Fig 10

Figure 10

Click here to access/download;Figure;Figure 10.pdf

A

B

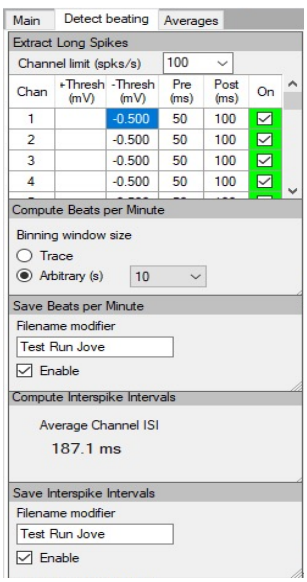

Fig 11

Figure 11

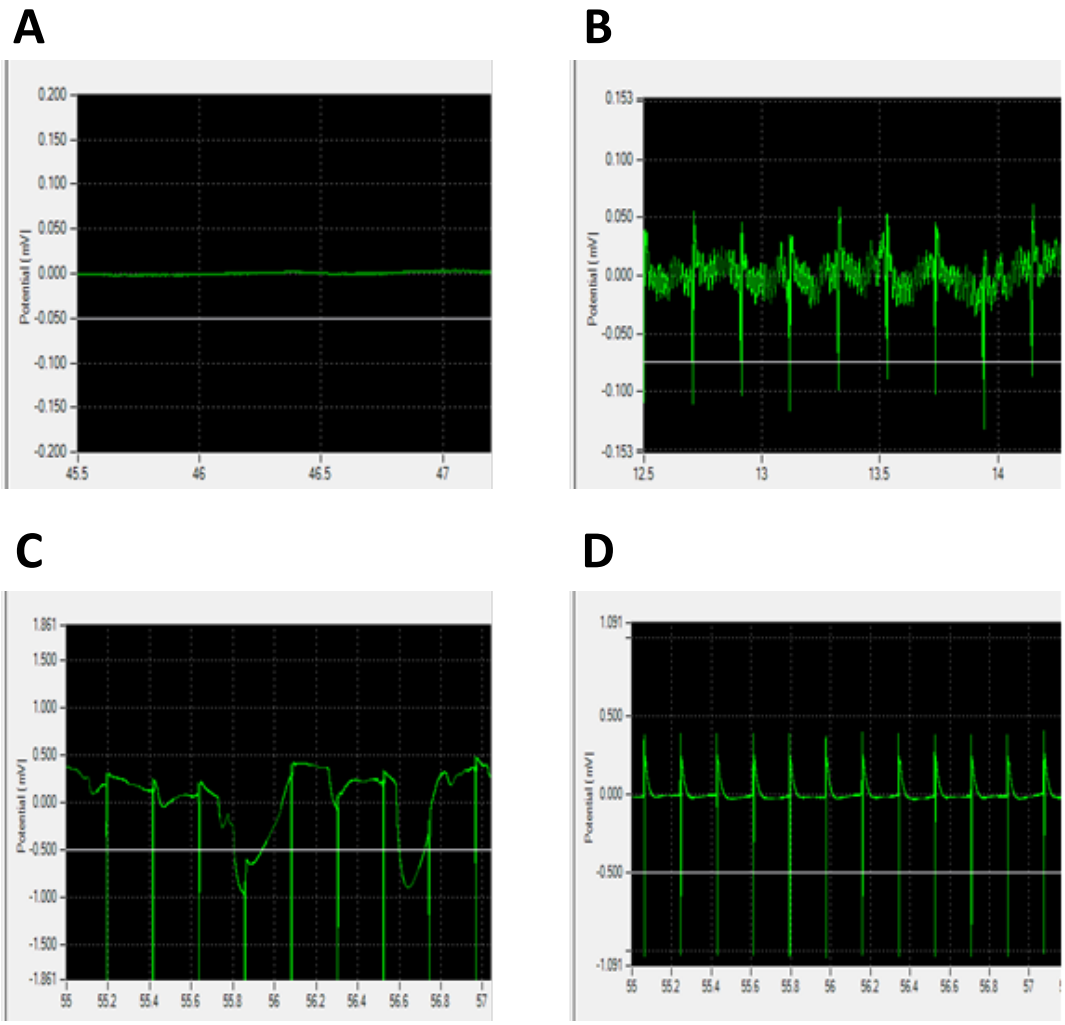

Figure 12

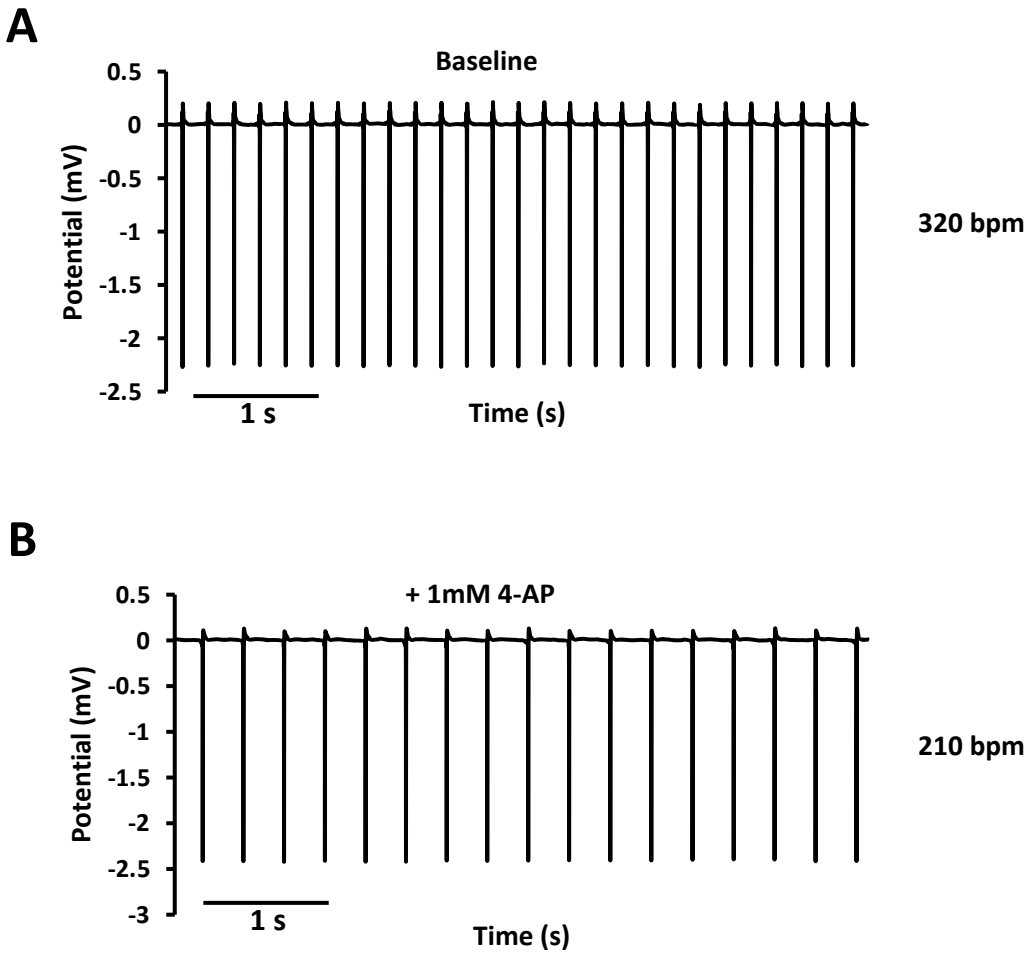

Name of Material/ Equipment	Company
4-Aminopyridine	Sigma
22 gauge syringe needle	Fisher Scientific
23 gauge syringe needle	Fisher Scientific
60mm Petri Dishes	Genesee Scientific
500mL Pyrex Bottle	Fisher Scientific
1000 mL Pyrex Bottle	Fisher Scientific
Bone Forceps	Fine Science Tools
Calcium chloride dihydrate ($CaCl_2 \cdot 2H_2O$)	Sigma-Aldrich
Carbogen (95% O_2, 5% CO_2)	
Castroviejo Scissors, 4"	Fine Science Tools
D-(+)-Glucose	Sigma-Aldrich
Data Acquisition PC	
Dissection Microscope	Jenco
Dissecting Pins	Fine Science Tools
Dumont #2 Laminectomy Forceps	Fine Science Tools
Dumont #55 Forceps	Fine Science Tools
Extra Fine Graefe Forceps	Fine Science Tools
Glass Chamber	Grainger
Harp Anchor Kit	Warner Instruments
HCl	Fisher Chemicals
Hemostat	Fine Science Tools
Heparin	Aurobindo Pharma Limited IDA, Pashamylaram
HEPES	Sigma-Aldrich
Inverted Microscope	Motic
Isoflurane	Patterson Veterinary
Lab Tape	Fisher Scientific
Light for Dissection Microscope	Dolan-Jenner
Magesium chloride ($MgCl_2$)	Sigma-Aldrich
MED64 Head Amplifier	MED64
MED64 Main Amplifier	MED64

MED64 Perfusion Cap	MED64
MED64 Perfusion Pipe Holder Kit	MED64
MED64 ThermoConnector	MED64
Mesh	Warner Instruments
Microelectrode array (MEA)	Alpha Med Scientific
Mobius Software	WitWerx Inc.
NaOH	Fisher Chemicals
Normal Saline	Ultigiene
Paint Brush	Fisher Scientific
Parafilm	Genesee Scientific
Peristaltic Pump	Gilson
Peristaltic Pump Tubing	Fisher Scientific
Polyethyleneimine	Sigma
Potassium chloride (KCl)	Sigma-Aldrich
Potassium phosphate monobasic (KH_2PO_4)	Sigma-Aldrich
Sodium Bicarbonate	Sigma
Sodium chloride (NaCl)	Fisher Scientific
Sylgruard Elastomer Kit	Dow Corning
Sodium Phosphate Monobasic	Sigma
Sodium tetraborate	Sigma
Surgical Scissors	Fine Science Tools
Transfer Pipets (3mL graduated)	Samco Scientific

Catalog Number	Comments/Description
A78403-25G	
14-826-5A	Used for dissection
14-826-6C	Used for dissection
32-105G	
06-414-1C	Used to store solutions
06-414-1D	Used to store solutions
16060-11	
C5080-500G	
15024-10	
G7021-1KG	
	CPU: Intel Xeon or Intel Core i7, Memory: 8GB, HDD: 1TB, Graphic Card: NVIDIA or On-board, Screen: 1920x1080
26002-20	
11223-20	
11295-51	
11152-10	
49WF30	Used for mouse euthanization
SHD-22CL/15 WI 64-0247	
SA48-4	Used for pH balancing
13013-14	
NDC 63739-953-25	
H3375-250G	
AE2000	
07-893-1389	
15-950	
MI150DG 660000391014	
208337-100G	
MED-A64HE1S	
MED-A64MD1A	

MED-KCAP01	
MED-KPK02	
MED-CP04	
640246	
MED-R515A	
	Specific software for the MED64
S320-500	Used for pH balancing
NDC 50989-885-17	
NC1751733	
PM-996	
F155009	
14-171-298	1/8'' Interior Diameter
P3143	
P9333-500G	
P5655-500G	
S6297	
S671-3	
184 SIL ELAST KIT 0.5KG	
S6566	
S9640	
14074-09	
225	

Name of Material/ Equipment	Company	Catalog Number

Comments/Description

RESPONSE TO REVIEWER AND EDITORIAL COMMENTS

We appreciate the detailed comments provided by the reviewers. Please find below our point-by-point responses to each comment. The corresponding changes to the manuscript have been denoted in red in the text.

Editorial comments:

Changes to be made by the Author(s):

1. Please take this opportunity to thoroughly proofread the manuscript to ensure that there are no spelling or grammar issues.

The document has been reexamined for spelling and grammar issues.

2. JoVE cannot publish manuscripts containing commercial language. This includes trademark symbols (™), registered symbols (®), and company names before an instrument or reagent. Please remove all commercial language from your manuscript and use generic terms instead. All commercial products should be sufficiently referenced in the Table of Materials and Reagents.
For example: Med64, parafilm, etc.

Med64 is removed as a keyword, Parafilm has been changed to thermoplastic film, and the silicone elastomer brand was removed from the text. The remainder of the article has been checked again for company names.

3. Please ensure that all text in the protocol section is written in the imperative tense as if telling someone how to do the technique (e.g., “Do this,” “Ensure that,” etc.). The actions should be described in the imperative tense in complete sentences wherever possible. Avoid usage of phrases such as “could be,” “should be,” and “would be” throughout the Protocol. Any text that cannot be written in the imperative tense may be added as a “Note.”

The document has been reexamined for proper tense usage throughout.

4. Please move the ethics statement before at the start of the protocol section before the numbered steps.

The ethics statement has been moved to beginning of protocol at lines 114-116.

5. Please include strain, age, sex of the animal used for the study.

Strain, age, and sex of the animal used in the study is on lines 529-530.

6. Please use the degree symbol - ˚C and do not use superscripted o.

All “˚C” have now been properly formatted.

7. For each step, please ensure you answer the “how” question, i.e., how is the step performed? e.g., how do you take a picture?

The document has been reexamined to ensure each step addresses the “How” question.

8. There is a 10-page limit for the Protocol, but there is a 3-page limit for filmable content. Please highlight 3 pages or less of the Protocol (including headings and spacing) that identifies

the essential steps of the protocol for the video, i.e., the steps that should be visualized to tell the most cohesive story of the Protocol.

Please find the requested text highlighted in the document.

9. Please ensure the results are described in the context of the presented technique. e.g., how do these results show the technique, suggestions about how to analyze the outcome, etc. The paragraph text should refer to all of the figures. Data from both successful and sub-optimal experiments can be included.

The results have been reexamined and meet the criteria described above.

10. As we are a methods journal, please ensure that the Discussion explicitly cover the following in detail in 3-6 paragraphs with citations:
a) Critical steps within the protocol
b) Any modifications and troubleshooting of the technique
c) Any limitations of the technique
d) The significance with respect to existing methods
e) Any future applications of the technique

The discussion has been reexamined and sufficiently answers these points.

Reviewers' comments:

Reviewer #1:

Manuscript Summary:
The submitted manuscript outlines in detail the methodology for isolating the murine right atrium, and performing multi-electrode array recordings from the SAN region. This is a well written manuscript that clearly outlines in great detail each step of the solution/equipment preparation, dissection, mounting the tissue, recordings, and analyses. This is a valuable tool that others in the field could benefit from this protocol. I have several critiques and items that need clarification.

Major Concerns:
* Abstract: "…without the influence of the autonomic nervous system" - this is not correct as the isolated heart removes external/central autonomic inputs, but the heart also includes intrinsic cardiac autonomic neurons that are sensitive to electrical and pharmacological stimulation. This topic is nicely reviewed in these 2 papers (PMC7712215 & PMC4808395) and in the detailed morphological and electrophysiological characterization by Dr. Dainius H. Pauza. The introduction and/or discussion would benefit from more detail about the autonomic inputs to the SAN.

This was a really great point to bring to our attention. We have read the recommended papers and added new content on lines 57-58, 81-82, and 676-678 to reflect these considerations.

* 3.4 & 6 What was the reason for the differences in the Tyrode's solution for tissue dissection vs. recordings? As the dissection solution is kept warm (37C) with 1.8 mM Ca2+, does the preparation keep beating (i.e., metabolically active)? If so, as the solution is not oxygenated, how to do you minimize ischemia?

Our MEA system is hooked up to carbogen so we designed our experiments and buffers to correspond to this setup. We prepared different Tyrode's solutions according to specifications in two different papers. The recording solution is referenced from doi: 10.1016/j.lfs.2008.06.020 and the dissection solution is referenced from doi: 10.3791/54555. The recording solution contains $NaHCO_3$ that needs the 5% CO_2 and 95% O_2 to maintain a pH of 7.4. The dissection solution contains 1.8 mM Ca^{2+} in 37C to keep the heart beating. The total time for dissection was brief, lasting only a few minutes such that ischemia should not significantly impact SAN tissue activity. The time for this tissue dissection is less than the total time to isolate single SAN cells which is usually done without oxygenation. Please see added text in lines 267-268 that addresses ischemia.

* 7.5 As cardiac beating rate and velocity of impulse propagation is extremely sensitive to temperature, please outline the methods for validating and maintaining spatially homogeneous 37C temperature control across the preparation. Are the solutions in the bottles and tubing kept at 37C?

The MEA system has temperature control built in to keep perfusion solutions at the set temperature (in our case 37C). The perfusion solution passes through the bottom of the platform where it is warmed to the set temperature before being introduced to the chamber with the tissue. A temperature sensor in the platform monitors and reports the actual solution temperature immediately before it enters the bath solution of the recording chamber.

* 10.2 When assessing the quality of the preparation, is there a minimum beating rate, minimum conduction velocity across the preparation, or maximum incidence/ratio of SAN-atrial exit block that is used to determine whether the preparation is healthy? The present definition of signal amplitude, as recognized by the authors, is very dependent upon tissue contact with the MEA, but does not fully confirm the health of the preparation.

We agree that other variables are important for assessing tissue health. The firing rate for healthy preps is about 300-330 beats/min which is similar to firing rates from patch clamp recordings. If it is lower than about 300 beats/min it may not be healthy for recording. We have now added this as a method to assess overall preparation quality in lines 540-541. In addition, we mention there that unstable variable firing rates are indicators of poor preps. As rightly pointed out, amplitude can be dependent on contact with the MEA, which we state in lines 523-524.

* 10.4 4-AP is a transient outward potassium channel blocker that is expressed in both the SAN and atria. As the focus of this protocol and study is on the SAN, it is advised to use a pharmacological agent in which the effects will be restricted to the SAN, such as the HCN blocker ivabradine. It is unclear whether 4-AP slows the beating rate of the preparation due to slowing SAN firing or SAN-atria exit block.

We agree that administration of an SAN drug such as ivabradine makes a lot of sense. However, here we only intended the focus of our demonstration to show that the system and recording paradigm is amenable to pharmacological interrogation. We chose 4-AP because we knew it was expected to have effects and we had it readily available in the lab, whereas we did not currently have access to ivabradine. To reflect this excellent idea to use more SAN region-specific drugs, we have included that as a future study idea in lines 682-684.

* For any drug study there should be a washout period to distinguish drug vs. preparation quality changes. This should be outlined and performed to characterize the stability of the preparation.

This is an excellent point to make in our protocol, and we have included it in lines 430-432.

* 9 The procedure for the data acquisition is written in a way requiring that the user have 1) All of the required files listed, and 2) All of those files have to be stored in the exact same location. These steps should focus more on what the file that is being opened does, and how to create these protocol files.

We have written the protocol to accompany the software and system referenced in the materials page, but this is a good point and we have now provided a note describing the acquisition steps more broadly in lines 366-368.

Minor Concerns:
* 6.10 The heart is bathed with 2-3mL of heparinized Complete Tyrode's solution. Is the heart submerged?

No, the heart is not submerged. We applied heparinized Complete Tyrode's solution to the heart using a dropper to keep the heart from drying out. We cannot completely submerge the heart tissue because it disrupts visibility during dissection. To make this point clearer we have added lines 260-262.

**7.4 "Set the peristaltic pump to 25 rpm'' What is the size tubing used to achieve 2mL/min?

The interior diameter is 1/8''. We have included this specification in the Materials List.

* 9.2 What are the acquisition settings (sampling rate)?

The sampling rate is 20kHz. We have added this detail at line 391.

* Discussion: "A tip to verify healthy and properly dissected SAN tissue is to examine it in Complete Tyrode's solution under the microscope as the SAN region should be clearly beating." SAN cells are not contractile, so the beating region is actually the atrial tissue.

We changed the text in line 653 to say that the "tissue is beating" rather than the "SAN tissue is beating." However, while weaker than some cardiac cells in the heart, the SAN cells do have contractile ability (see this article for reference: https://doi.org/10.1152/ajpheart.00068.2015)

* Figure 4 - please move the IVC and SVC labels closer to those landmarks/vessels.

Please see the revised Figure 4 for clearer labeling.

Reviewer #2:
Manuscript Summary:
The study provides a regular approach to test the electrophysiology of sinus node (SAN) tissue by MEA. MEAs are composed of multiple microelectrodes arranged in a grid-like pattern for recording in vitro extracellular field potentials. They present a methodology to measure the electrophysiology of SAN tissue by performing microelectrode array (MEA) recordings. However, some defects exist in the manuscript.

Major Concerns:

1. The preparation of the MEA grid and the physical characteristics electrode are not well described.

Please see lines 134-138 and Fig 1 for an in-depth description of the MEA and electrodes.

2. Considering that the Tyrode's solution is a phosphate buffer system, but not a carbonate buffer system, carbogen is not necessary for oxygenating the Tyrode's solution. Pure oxygen might be better for maintaining the suitable oxygen content and pH of the Tyrode's solution.

Our recording solution contains $NaHCO_3$ which requires the carbogen in order to maintain the pH. The dissection solution utilizes the phosphate buffer system and is used in our lab with pure oxygen as you describe for other electrophysiology methods. Please see lines 159-166 and 182-184 for the components in the dissection and recording solution, respectively.

3. Can the authors add the data demonstrating the survival time of the isolated SAN tissue.

We have added survival time information in lines 514-515.

4. The DATA recorded by MEA should be further analyzed. Besides the firing rate, demonstration of the Field potential duration (showing the repolarization), activation map (showing the electrical conduction), conduction velocity, phase map, pacemaker point, etc will help a lot for the improvement of the significance of this methods study.

These are good ideas that we have not yet been able to rigorously optimize with our system. However, since our system should be theoretically capable of looking at the parameters mentioned in this comment, we have mentioned some of these in the discussion as other possible applications of this technique. Perhaps these applications would make a nice follow-up methods article. Although field potential duration has been measured in another paper doi: 10.3233/BME-151380 that used a different dissection method from ours, we do not think it represents a reliable measurement in this method since it could potentially vary between preps based on electrode placement.

5. As an inhibitor for potassium channel, 4-AP might mainly have an effect on the repolarization stage of the action potential, but not the firing rate (sometimes 4-AP might increase the beating rate of pacemaker cells). Thus, to evaluate the firing rate, Ih inhibitor (ivabradine), RyR inhibitor (Ryanodine) or PKA inhibitor (H89) might be more effective and representative to decrease the beating rate of the isolated SAN tissue.

As mentioned to Reviewer 1 above, we agree that administration of an SAN drug such as ivabradine makes a lot of sense. However, here we only intended the focus of our demonstration to show that the system and recording paradigm is amenable to pharmacological interrogation. We chose 4-AP because we knew it was expected to have effects and we had it readily available in the lab, whereas we did not currently have access to ivabradine or Ryr or PKA inhibitors. To reflect this excellent idea to use more SAN region-specific drugs, we have included that as a future study idea in lines 682-684.

Minor Concerns:
The position of the label in Figure 4B ("SVC", "IVC") should be described more precisely. Arrows will be helpful for indicating the anatomic location of the "SVC" and "IVC".

Please see the revised Figure 4 for clearer labeling

Reviewer #3:
Manuscript Summary:
This manuscript by Kumar et al describes a protocol for recording spontaneous activity of the dissected but intact sinoatrial node of the mouse heart using a microelectrode array (MEA). The protocol is clearly written and easy to follow. The notes on different steps of the protocol are particularly useful. The overall idea of using MEAs for assessing intrinsic SAN activity is likely to be useful in some applications. The lovely representative data showing the effects of 4AP perfusion (Fig 12) are very convincing.
The protocol would be more useful if it included details of the specific MEA and software used. Perhaps this information was not included due to journal policy, but since such information is essential for the utility of the protocol and it would seem to warrant an exception to the policy. The manuscript would also be improved by expanded discussion of limitations of the approach.

Major Concerns:
1. What specific MEA hardware and software is used in the protocol? It would be ideal to provide procurement info, range of costs, and a brief comparison of pros and cons of different units. As it stands, the steps and figures that describe the specific software used in the protocol are not particularly informative if the software is not identified. If journal policy prohibits identification of the hardware and software, consider deleting or generalizing the information in steps 9-10 and the corresponding figures (7-10).

The software and specifications for this MEA can be found in the materials list that is provided with the article. We have added a note that references generalizability of the steps in lines 366-368. We have added lines 690-691 to describe availability and general cost of MEA systems.

2. Given that beating rate/interspike intervals are usually the same in all channels, what is the advantage of using a MEA compared to a single extracellular electrode? And, why is it necessary to make sure that all electrodes in the array have a signal? Can the impulse initiation site and conduction velocity through the small mouse SAN be resolved from differences in response time of different electrodes?

1) MEA advantages: The single extracellular electrode recordings require much more specialized electrophysiological technical expertise. Also, using the MEA allows for multiple recording sites at one time which provide broader coverage in case differences do exist between different sites in the tissue.

2) It is not necessarily mandatory to make sure all electrodes have a signal, but it is a good way to ensure good contact is being made across the tissue and that all of the tissue within the MEA is healthy.

3) It should be theoretically possible to identify impulse initiation site and conduction velocity using this system, but we have not attempted or optimized that technique yet, so we do not feel qualified to discuss it, let alone provide instructions on how to do it.

3. Although the MEA approach is likely to be useful in some applications, the limitations of the approach should be better acknowledged and discussed. For example, how might problems or differences in conduction (e.g., in different preps or due to drugs) interfere with determination of a single firing rate for a prep? Might there be cases of two competing impulse initiation sites, particularly at slower FRs? Along the same lines, it seems that inclusion of atrial tissue in the

prep would alter the firing rate of the SAN itself. Of course, this condition is also present in vivo, so it is not necessarily a limitation, but it's also not clear that the dissected SAN prep eliminates mechano-electric mechanisms as stated (e.g., lines 647-649).

We have included additional discussion of limitations regarding measuring action potential characteristics with an MEA, as well as potential confounding influences of autonomic innervation, in lines 675-679 and 692-695. As we now state, the MEA can only record field potentials which is less precise than the intracellular action potential recordings for measuring action potential characteristics. Regarding mechano-electric mechanisms, sinus firing rate can be variable due to mechano-electric mechanisms related to ventricular contraction and respiration, suggesting reentrant signals can occur with an entire heart with an intact conduction system. However, in our recordings these mechano-electric effects should be minimal since the only tissue present in the preps is SAN tissue and part of right atria.

4. It should also be mentioned that movement artifacts of the spontaneously beating SAN may limit the usefulness of the MEA approach. This appears to be the case in Fig 11C. How frequently is this type of noise observed? When present, does it affect all electrodes and does it necessarily preclude assessment of firing rate?

Fig 11C was a rare example of an unstable recording. We did not find any issues with movement artifacts, perhaps because the electrodes are stably in contact with the tissue.

Minor Concerns:
1. Lines 50-51. Intrinsic heart rate not clearly defined.

We have added a definition of intrinsic heart rate in lines 50-52.

2. In reference to Fig 8, it is stated that APs may not be aligned across channels (lines 498-500) but this cannot be resolved in Fig 8.

It is not obvious in Figure 8, but there can be minute (ms scale) differences in alignment. The differences are so small it is difficult to display the alignment clearly in a figure.

3. Lines 504-505. How was the minimum acceptable amplitude of 0.5 mV determined?

From extensive personal experience with the system, we have learned that healthy tissue tends to average at least 0.5mV signal amplitude.

4. It sounds as if episodic recording was used in the example recordings. Why not use continuous recording?

Because we record 64 channels at a 20 kHz sampling rate, the file sizes get unmanageably large very fast so continuous recording is not feasible.

5. Line 653-655. How would stimulation of SAN be relevant physiologically? And what types of arrhythmias might be measured in SAN?

We removed the lines discussing stimulation because we intended it to refer to stimulation of other cardiac regions outside the SAN and upon re-reading, we removed it due to ambiguity.

*6. The SAN dissection (e.g., Figs 2-4) has previously been described by several groups and such references should be cited.

Lines 85-87 reference such articles.

7. Fig 11 showing some examples of poor data is informative. What percentage of preps are adequate for recording once the dissection has been mastered? Can some of these problems be corrected, say by repositioning the tissue on the array? Is noisy data in some channels necessarily present in all channels?

Once the dissection has been mastered, more than 90% are good for recording. We have included this information in lines 654-655. In our experience, if one channel has noise, several will also have noise because the problem is usually systemic. One exception is if you have had an electrode go bad in which case you would not get a signal at all. Repositioning the tissue typically does not resolve problems with noise but can be used to realign the region of interest with the desired electrodes.

8. p 35-38. The list of equipment and details are poorly formatted and difficult to interpret. Perhaps this information was presented in a table in the original file?

The original file is an excel sheet table which should be more clear in the published article.